

NASA
CR
2997
c.1

NASA Contractor Report 2997

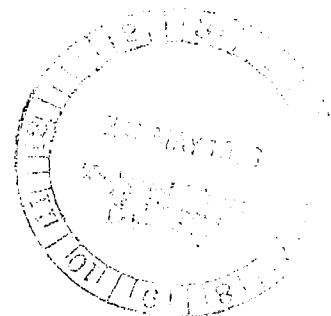
LOAN COPY - RETURN TO
AFWL TECHNICAL LIBRARY
KIRTLAND AFB, NM

TECH LIBRARY KAFB, NM
0061640

Atmospheric Scavenging of Solid Rocket Exhaust Effluents

Donald L. Fenton and Robert Y. Purcell

CONTRACT NAS8-31947
APRIL 1978





NASA Contractor Report 2997

Atmospheric Scavenging of Solid Rocket Exhaust Effluents

Donald L. Fenton and Robert Y. Purcell
IIT Research Institute
Chicago, Illinois

Prepared for
George C. Marshall Space Flight Center
under Contract NAS8-31947



National Aeronautics
and Space Administration

**Scientific and Technical
Information Office**

1978

FOREWORD

This document is the final report on IITRI's Project No. C-6365 entitled "Atmospheric Scavenging Exhaust" and was performed under NASA Contract No. NAS8-31947 from the Marshall Space Flight Center. The report presents and discusses the rocket exhaust HCl scavenging data and the auxiliary experiments conducted.

The authors enthusiastically acknowledge the numerous suggestions and support from the project monitor, Dr. J. Briscoe Stephens, at the NASA Marshall Space Flight Center. The rocket motors used to generate the exhaust cloud were obtained from the Jet Propulsion Laboratory, where the assistance of Mr. Leon Strand was especially important. Guidance from Mr. Keith Dumbauld of Cramer Co. was important in modeling the experimental data.

At IITRI, Dr. E. L. Grove painstakingly carried out the chlorine-ion analysis and is gratefully acknowledged for this work. Mr. Harry Nichols and Mr. Vernon Hill of IITRI's Metals Division designed and conducted the metallic corrosion tests. Dr. Manfred Ruddat, a botanist at the University of Chicago, served as a special consultant relating to HCl plant uptake and growth response.

TABLE OF CONTENTS

	<u>Page No.</u>
1. INTRODUCTION	1
2. EXPERIMENTAL APPARATUS	2
2.1 Aerosol Chambers	2
2.2 Rocket Motor and Exhaust Cloud	9
2.3 Rain and Fog Simulation	10
2.4 Rain Collection	18
2.5 Measurement of Hydrogen Chloride Concentration	19
2.6 Absorption Chamber	31
2.7 Growth Chamber of Experimental Plants	39
2.8 Metallic Coupons	42
3. EXPERIMENTAL PROCEDURE	44
4. EXPERIMENTAL TEST DATA AND RESULTS	47
4.1 Scavenging Test Results	
4.1.1 Rocket Exhaust HCl Scavenging Data	47
4.1.2 Correlation of Scavenging Data	51
4.2 Absorption Tests	54
4.3 Plant Uptake Tests and Growth Response	56
4.4 Metallic Corrosion Tests	60
4.5 Characterization and Scavenging of Rocket Exhaust Aluminum Oxide Dust	64
5. CONCLUSION	70
References	76

LIST OF FIGURES

		<u>Page</u>
1	Experimental Apparatus	3
2	Support Frame for Teflon Comprising Test Chamber . .	5
3	Photograph of Completed Experimental Chamber	6
4	Assembly Detail of Diluter/Transport System	8
5	Rocket Motor Mounting within 5.49 m (18 ft) Spherical Chamber	11
6	Data Sheet for Experimental Test Rocket	
7	Raindrop Generator	15
8	Raindrop Receptacle	20
9	Liquid Calibration Response for the IITRI HCl Detector	24
10	Liquid Calibration Response for the Langley HCl Detector	25
11	Calculation Results for Droplet and Gaseous Diffusion of HCl Showing Theoretical Magnitude of Separation	28
12	Schematic Diagram of Air-Dilution System	30
13	Design of Duct for HCl Absorption Experiments . . .	35
14	Schematic Diagram of Equipment Used in Preliminary HCl Absorption Experiment	37
15	Surface Absorption Flux of HCl to Distilled Water Versus Mean Gaseous HCl Flux Above Surface	40
16	Plant Growing Chamber	41
17	Corn and Soybeans (behind corn) Responding to Conditions Inside Growth Chamber	43
18	Rocket Exhaust HCl Scavenging Data for Multiple Raindrop Sizes	49
19	Raindrop Terminal Fall Velocity as Determined by Gunn and Kinzer	52
20	Rocket Exhaust HCl Deposition Velocity Variation with HCl Concentration	57
21	Growth Response of Soybean Seedlings Two Weeks After Germination	61
22	Net Coupon Weight Changes Versus Length of Exposure Time	62
23	Al ₂ O ₃ Particle Size Data for Second Scavenging Test	66
24	Al ₂ O ₃ Particle Size Data for Third Scavenging Test .	68
25	Al ₂ O ₃ Particle Size Distributions Based on Number for Both Airborne and Collected Rain	69
26	Photomicrographs Showing Al ₂ O ₃ Particles Collected by 1.1 mm Raindrops at 3,000X Magnification . . .	71
27	Photomicrographs Showing Al ₂ O ₃ Particles Collected by 1.1 mm Raindrops at 10,000X Magnification . . .	71
A-1	Pure HCl Scavenging Data for Multiple Raindrop Sizes	75

LIST OF TABLES

	<u>Page</u>
1 Raindrop Generation System Characteristics	17
2 Scale Factor Calibration for the HCl Detectors	22
3 Composition of Laboratory Sea Water	32
4 Preliminary Test Results for Absorption Chamber	38
5 Materials for Corrosion Test Matrix	45
6 Droplet Scavenging Results for Rocket Exhaust HCl	48
7 Rocket Exhaust HCl Absorption Test Results	55
8 Summary of Test Plants HCl Uptake Measurements	59
9 Measured Weight Changes Associated with Exposed Metal Coupons	63

ATMOSPHERIC SCAVENGING EXHAUST

1. INTRODUCTION

An assessment of the environmental effects associated with the ground exhaust cloud formed during the initial phase of a Space Shuttle launch is important because a major constituent of the exhaust cloud is hydrogen chloride. It is well known that hydrogen chloride can be potentially toxic depending on the local circumstances.

Investigations conducted recently at both NASA-Langley and IITRI determined the extent of HCl washout for rain storms typical of the Cape Kennedy launch area. However, this early work left a serious gap concerning the scavenging of rocket exhaust HCl. Pellet (1) at NASA-Langley conducted very careful experiments with pure gaseous HCl and the data obtained supported the Frossling correlation. Knutson and Fenton (2) at IITRI conducted experiments utilizing real solid-propellant rocket exhaust but limited the conditions to relatively high HCl concentrations and a single droplet size. The goal of this work, then, was to fill the gap -- experimentally evaluate actual rocket exhaust HCl scavenging under typically encountered conditions for varying raindrop sizes. Auxiliary experiments were conducted to determine absorption rates or "uptake" of HCl for a range of materials including plant-life and liquids common to the launch site. In addition, corrosion studies were performed on a representative set of metallic coupons.

Modifications in the test apparatus were necessary to facilitate multiple HCl scavenging and absorption experiments. These changes greatly expanded the information obtained. The modifications included limiting the large, spherical chamber for the sole purpose of storing the exhaust cloud constituents generated by the test rocket. A second experimental chamber, much smaller in volume, served as the location for all the experimental activity.

After the exhaust cloud has formed and reached the terminal altitude, prevailing winds cause the cloud to drift and local wind shear and atmospheric turbulence cause cloud dispersion. The stage of cloud history is predictable by the NASA/MSFC multi-layer diffusion models (3). These models permit taking into account a number of meteorological parameters and allow stratification of the atmosphere. The multi-layer diffusion models have a provision for calculating precipitation scavenging of HCl from the ground exhaust cloud. The required input for HCl scavenging is the washout coefficient -- a function of only the rain intensity.

2. EXPERIMENTAL APPARATUS

The thrust of this study was the determination of the HCl scavenging rates from a rocket exhaust cloud at concentrations typical of the ground exhaust cloud. Small-scale rockets ignited within a large, spherical chamber generated the exhaust cloud, which, at appropriate times, was transported to a second, small chamber constructed of Teflon. This second chamber is where all the experiments were conducted. In this way, the HCl concentration was sufficiently diluted to achieve the necessary low concentrations. The remaining experimental equipment included the rain simulator, fog nozzle, rain collector, absorption chamber, and plant growth chamber. The purpose of all this equipment was to confine the exhaust cloud in order to carry out the meaningful measurements and characterize the exhaust cloud. Special instrumentation was used to monitor the HCl concentration within the cloud and measure the particle size distribution of the Al_2O_3 dust.

2.1 Aerosol Chambers

Two chambers were used to perform the scavenging and uptake tests for HCl. The first chamber (large sphere) was used to store the exhaust gases after the test rocket was ignited. The second chamber (Teflon bag) was the location of all the experimental activity except surface absorption. Figure 1 is a schematic diagram depicting the major components of the experimental system.

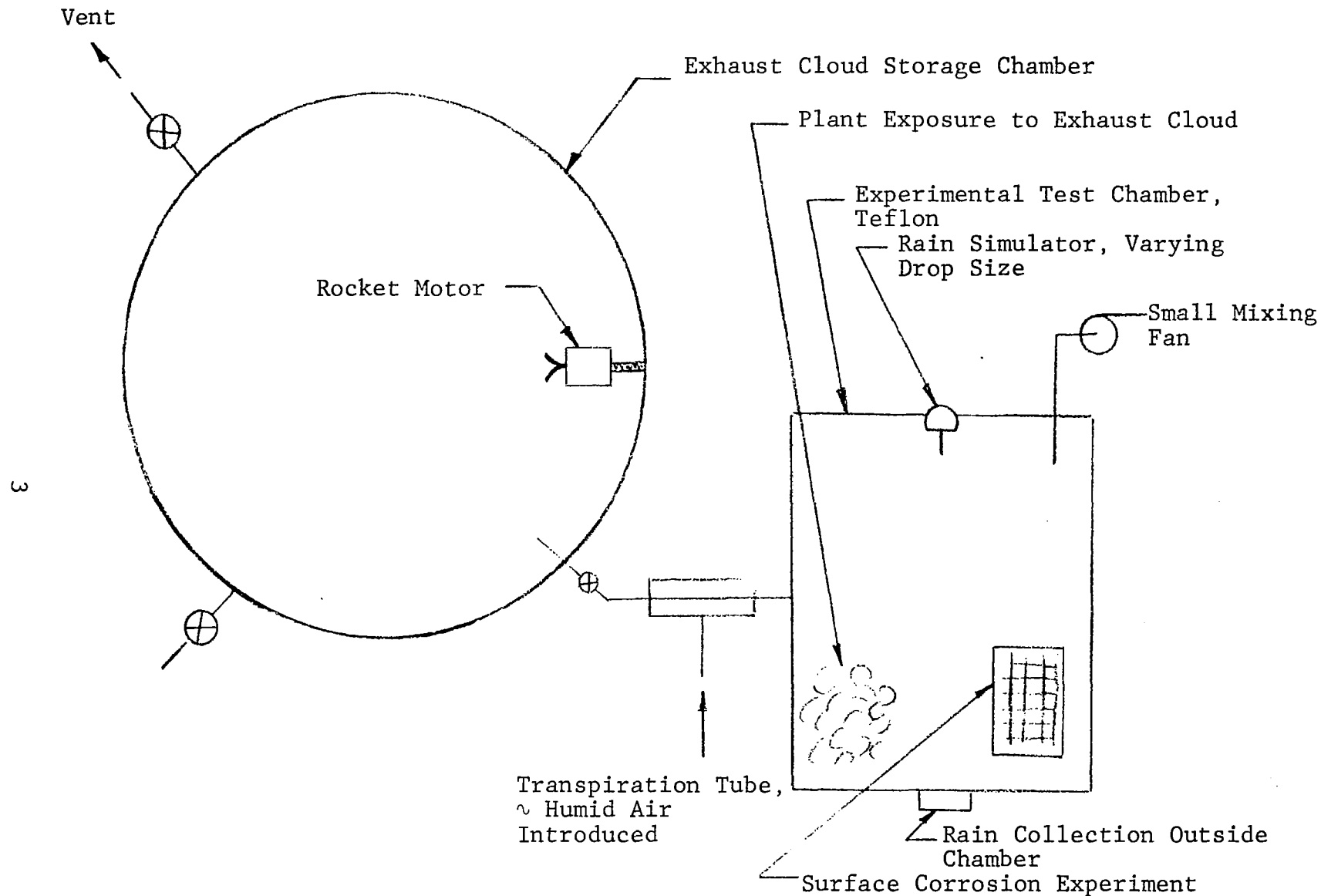


Figure 1

EXPERIMENTAL APPARATUS

The spherical chamber was fabricated from welded steel plate and is 5.49m in diameter. This chamber is rated for 5.44 atmospheres of gauge pressure and has a calculated volume of 86.5m^3 . The inner surface of the chamber was coated with Plasite #7122, an epoxy-phenolic material resistant to acids, and an oil-base enamel. A wash-down spray head was installed at the top of the chamber to clean the chamber after each rocket ignition. The rocket motor was secured to the chamber wall by means of a stud fastened to a modified port. The chamber was also fitted with an exhaust system that when operated maintained a negative pressure within, permitting evacuation of the contents. Evacuation was performed at the conclusion of each test.

The second chamber, where the scavenging experiments were performed, has an available rocket exhaust cloud supply over a period of several hours. This time interval was deduced from HCl concentration decay and coagulation rates of the Al_2O_3 dust. The significance of the second "experimental" chamber is that it afforded convenient control over the exhaust cloud concentrations tested and permitted multiple tests for one rocket firing.

The material used in the construction of the experimental chamber was FEP Teflon film* (.0127 cm thick) and modified on one side to accept special adhesives. The experimental chamber was essentially a bag, and therefore required external support. Figure 2 gives the outside dimensions of the frame used to support the bag. The bag was made to contour the basic rectangular shape of the support frame by glueing the Teflon sheets in a way to locate the unmodified surface on the inside of the bag. A removable door, 61 cm square, was provided to change experiments within the experimental chamber for any one rocket firing. The door was designed utilizing a special rubber gasket to provide a tight seal with the remainder of the test chamber. A plywood floor was located under the lower surface of the bag in order to support test equipment within the experimental chamber. Figure 3 shows a photograph of the completed experimental chamber.

*Cadillac Plastic and Chemical Co., Dallas, Texas

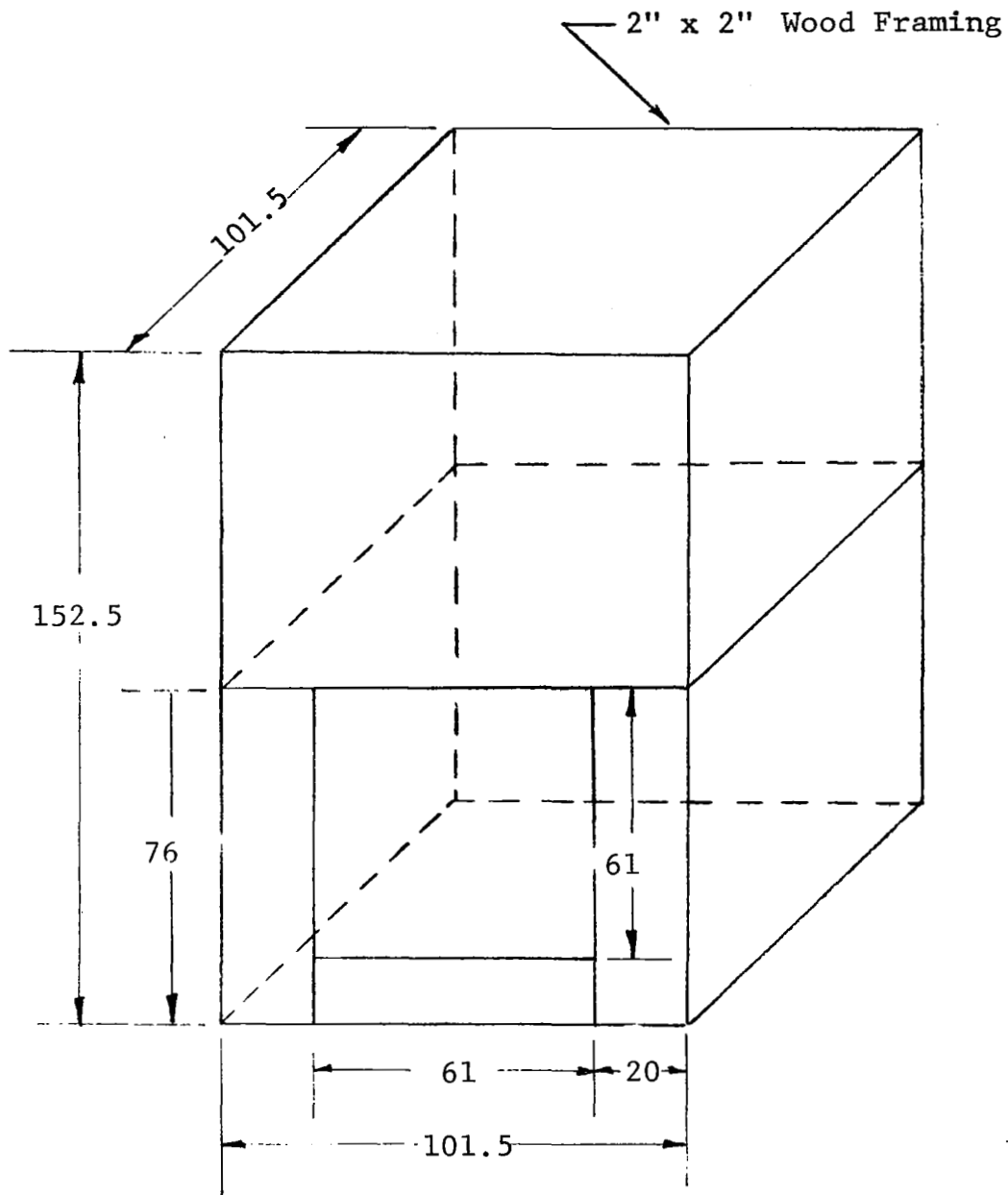


Figure 2

SUPPORT FRAME FOR TEFLON COMPRISING TEST CHAMBER

Note: All dimensions in cm.

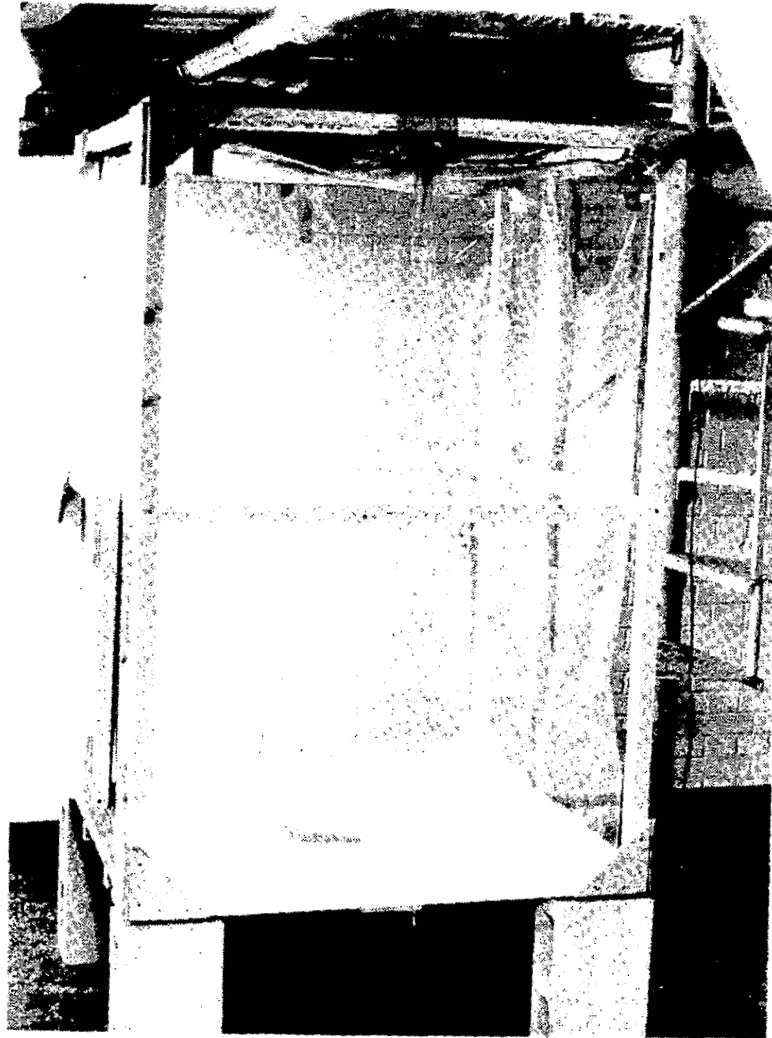


Figure 3

PHOTOGRAPH OF COMPLETED EXPERIMENTAL CHAMBER

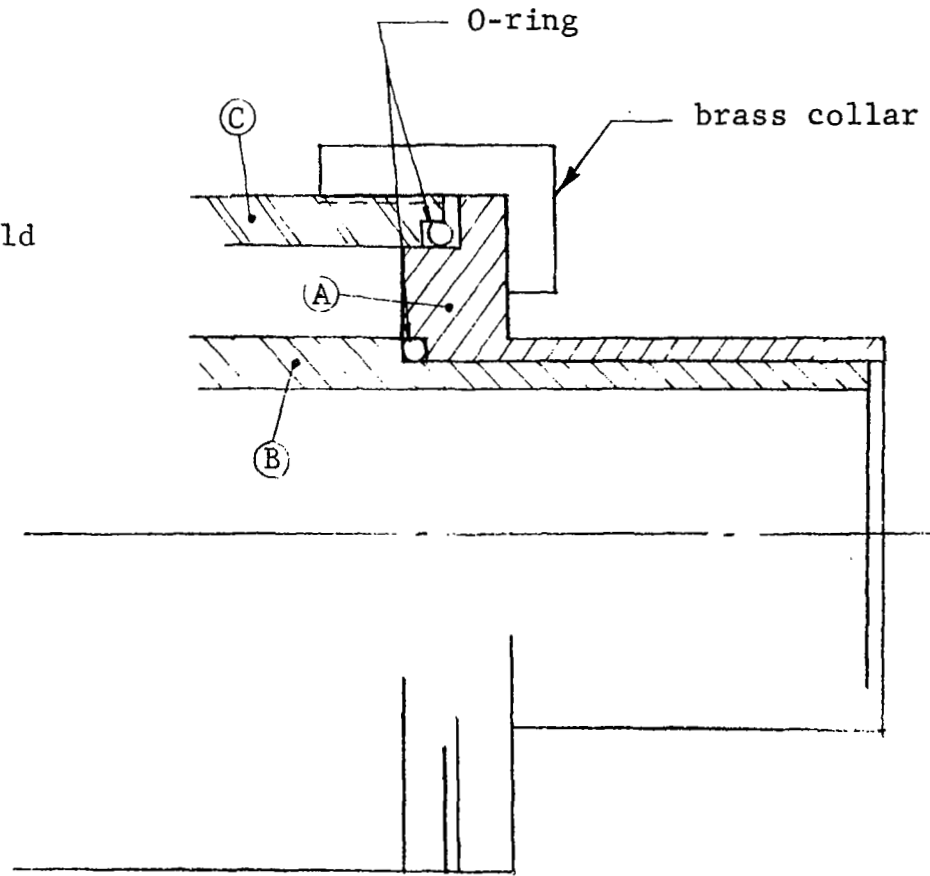
One problem arose with glueing certain sections of the experimental chamber. The Teflon film was modified on one side to accept and hold a glueing compound while the opposite side would not. An etching kit was used to modify the untreated side so that glueing could also be achieved, thus enabling the construction of the experimental chamber with a door and still maintaining a complete enclosure of Teflon. The etching technique did not function properly. A series of other adhesives were attempted and one, Fluoro-Plastic adhesive #30, was found satisfactory. This adhesive is a pressure sensitive contact glue for binding Teflon and other plastics.

The successful use of the experimental chamber necessitates the efficient transport of the rocket exhaust from the spherical chamber to the experimental chamber. A specially designed transport tube was installed to minimize wall losses of both HCl and Al_2O_3 . The concept used in the transport incorporates transpiration air introduced along the length of the tube. This concept has been used by Ranade (4) with good success to transport aerosols in other applications. The transpiration air sheath, which permits the efficient transport of the aerosol, was generated by supplying air via a manifold (4 parts along total 46 cm. length) along a porous tube. Figure 4 is a diagram showing the assembly details of the dilution/transport system.

To accomplish the transport of the exhaust from the spherical chamber to the experimental chamber, the negative pressure generated by laboratory's exhaust fans was utilized. PVC pipe and valves were used to transport and regulate the rocket exhaust to the experimental chamber. The expelled exhaust was transported via a flexible 5 cm. hose to the laboratory's air filtration box which provides the source of vacuum. Special internal bag supports coated with epoxy-resin paint and glued wood slats prevented the bag from collapsing upon discharge.

A fan was installed inside the experimental chamber to provide good mixing of the bag's contents. The fan itself was fabricated from sheet steel and bolted to a steel shaft. Both the

- A - Porous tube spacer
- B - Porous tube
- C - Outer shell manifold



8

Figure 4
ASSEMBLY DETAIL OF DILUTER/TRANSPORT SYSTEM

fan blades and shaft were coated with epoxy-resin paint to minimize HCl absorption and consequent corrosion. The Teflon bag provided a seal as the hole was slightly smaller than the shaft diameter. The driving motor had a variable speed control thus providing numerous levels of agitation. The fan blade length was approximately 10 cm and the shaft length roughly 40 cm. With the introduction of fog, the mixing action was observed to vary from mild to vigorous.

2.2 Rocket Motor and Exhaust Cloud

The rocket motors used to generate the exhaust cloud within the spherical chamber were obtained from the Jet Propulsion Laboratory in Pasadena, California.* Each rocket motor contained approximately 0.277 kg bonded-in propellant grain, with a 5.19 cm diameter axial perforation. The propellant outside diameter was 7.6 cm while the length was 5.16 cm. The propellant composition was as follows (5):

Ammonium perchlorate	70% by weight
Aluminum	16%
PBAN	14%

Minor constituents of the propellant grain were changed from the previous scavenging experiments (2). One modification included the addition of about 0.1 to 0.2 percent iron oxide to regulate the burning rate of the rocket motor. In this study, iron oxide was shown, through particulate sizing of the exhaust cloud, as not influencing the overall particle loading or particle size distribution. Other trace constituents were also modified; but, because of their low concentrations, they are not considered significant for scavenging experiments.

The rocket exhaust gases discharged through a converging-diverging nozzle with an expansion ratio of 4:1 and a throat diameter of 0.927 cm. A spent rocket mounted within the cham-

*Arrangements for the delivery of these rockets to IITRI were made by Dr. J. Briscoe Stephens and Mr. H.R. Hope of NASA/George C. Marshall Space Flight Center and Mr. Leon Strand of the Jet Propulsion Laboratory. Pertinent JPL drawings are D9041893 and D9041612.

ber is shown in Figure 5. A typical trace of the rocket motor combustion chamber pressure is displayed in Figure 6. During the test rocket burn, the chamber pressure rise was sufficiently rapid to permit the generation of typical exhaust constituents. Among all the pressure traces received, burn time variations were observed on the order of 10-15%.

As the spherical test chamber contained approximately 102 kg of air prior to rocket ignition and the rocket 0.227 kg of propellant, the dilution factor within the spherical chamber was approximately 450 on a mass basis. Assuming that all the chlorine goes to HCl and all the aluminum goes to Al_2O_3 , the following initial concentrations in the spherical chamber were expected (not measured):

HCl:	49.1g,	0.567 g/m ³ ,	, 386 ppm (volume basis)*
Al_2O_3 :	68.7g,	0.794 g/m ³ ,	

In the above calculated concentrations, after-burning was considered to be complete.

2.3 Rain and Fog Simulation

The method of raindrop generation used produces uniformly sized drops. This enables the determination of the HCl scavenging rate for a specific raindrop size. With the HCl scavenging rate varying with droplet size, the effective scavenging rate for a particular rainstorm can be found by knowing the raindrop size distribution. This method of approach is taken because it is not feasible in the laboratory to duplicate a natural rain in both droplet size distribution and intensity. Rain intensities are relatively simple to control if droplet size is disregarded. However, the HCl scavenging rate per raindrop is not a function of rainfall intensity, but of the complicated mechanisms of HCl-H₂O mass-exchange-rates at the surface which is influenced by raindrop size.

*Standard dry conditions

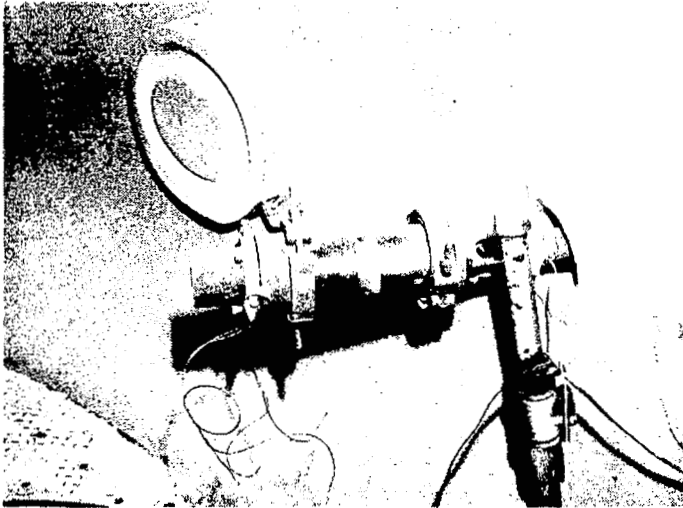


Figure 5

Rocket Motor Mounting
within 5.49 m (18 ft) Spherical
Chamber.

Photo taken after firing.
Note white Al_2O_3 dust on
upward facing surfaces.

Rocket housing diameter
is 7.5 cm (3 inches).

Engineer

JET PROPULSION LABORATORY

Batch No. LS-69

L. Strand

LOADING DATA FOR CASE BONDED
INTERNAL BURNING TUBULARS
OR 2-5071A STAR

Charge No. 10

Job No. 365-40501-0-3450

Date Cast 7-22-76

By Gurak-Ford-Tervet

PROPELLANT

PLUGS

No. LS-69 Mixer _____ No. ECCOBOND45
 Viscosity _____ Temp., °F _____ Viscosity _____ Temp., °F 16
 Remarks: _____ Remarks: _____

WEIGHTS (gms.)

- 1. Weight after adding end plugs (total weight). 1902
- 2. Weight after machining to length. 1896
- 3. Weight of plugs (1-2). 6
- 4. Weight of empty chamber. _____
- 5. Weight of propellant (2-4). _____

DIMENSIONS (inches)

- 1. Length of chamber. 6
- *2. I.D. of chamber. 3
- *3. Diameter of axial perforation (tubulars only). 2.042
- *4. Diameter of inner star point circle (star only). _____
- *5. Length of propellant after machining. 2.03
- 6. Length of propellant plus plugs. _____
- 7. Thickness of plugs (6-5). _____

TEMPERATURE HISTORY

MONTH	7							
DAY	22							
HOUR	12:30							
TEMP., °F	160°							
CURE	4DA							
COOL	7-26							

Figure 6

DATA SHEET FOR EXPERIMENTAL TEST ROCKET

Test Temp., °F 80°

Date 6/1/77

Observer D. Fenton

JET PROPULSION LABORATORY
SOLID ROCKET TEST DATA

Run No. _____

Batch No. LS-69

Charge No. 10

Job No. C6365

Engineer P. Ase

Propellant No. LS-69-10

Purpose of Test Obtain rocket exhaust products in 18 ft. diameter space for study

Internal Tubular _____ Star _____ Special _____

Igniter Type JPL 540 Igniter Lot No. _____ Wt., gms. 6.5 g

Squibs Nichrome wire

Safety Diaphragm: Metal _____ Thickness, in. _____ Dia., in. _____

Nozzle Type JPL-D9041893 4:1 expansion nozzle

Transducers PCB Model 113A24 ~ 5mv/psi Scope Tektronix 551

Power Supply PCB Model 482A, output neg. Calibration overall, 0.5 sec/cm

Charge Ampl. Kistler 556 - 10mv/pcb Photo taken 2v/cm trace on scale-200 psi/cm

1v/cm trace off scale-100 psi/cm

Remarks: Two traces were used with different sensitivity to catch one on scale.

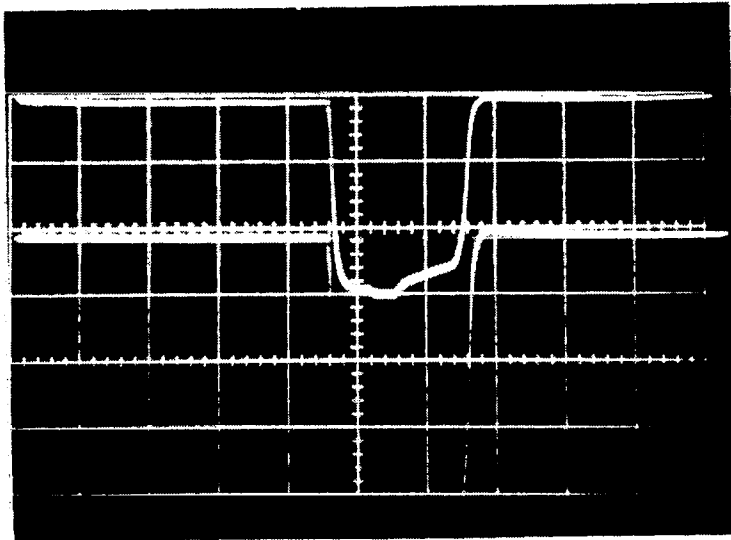


Figure 6 (continued)

The experiments evaluated the scavenging of HCl under multiple raindrop sizes. A rain generation system was selected on the basis of the capability to produce uniformly sized drops. The method of raindrop generation was important as drop size enters directly into the calculation for scavenging rate.

The raindrop generation system used is based on the capillary instability principle for producing uniformly sized drops. This system provides the advantage of control of both raindrop diameter and initial fall velocity. The liquid jet break-up resultant of capillary instability was theoretically developed by Lord Rayleigh in 1878 (6). His development shows that a laminar, low-viscosity, liquid jet is inherently unstable due to surface tension and tends to amplify longitudinal disturbances of a definite wavelength, λ , equal to 4.508 times the jet diameter, D_j . As these waves increase in amplitude, the jet breaks into equal-sized segments. The resulting drop diameter, D_d , is therefore 1.89 times the diameter of the jet. The equations for Rayleigh break-up are as follows:

$$\begin{aligned}\lambda &= 4.508 D_j \\ D_d &= 1.89 D_j \\ F &= V_j / \lambda\end{aligned}$$

where F is the applied frequency of excitation and V_j is the velocity of the emerging liquid jet.

Investigations relating to Rayleigh's work have determined that the production of mono-dispersed droplets was achieved for λ/D_j ratios varying from 3.5 to 7.0 (7, 8, 9, 10). This range in the λ/D_j ratio was determined from empirical measurements.

The raindrop generator consisted of a square-ended (carefully machined) hypodermic needle mounted on an acoustic transducer. An ordinary audio oscillator was used to drive the transducer and therefore perturb the liquid jet. Figure 7 is a schematic diagram showing the components of the raindrop generation system. The water reservoir was a large polyurethane bottle filled approximately to one-half the total volume with distilled

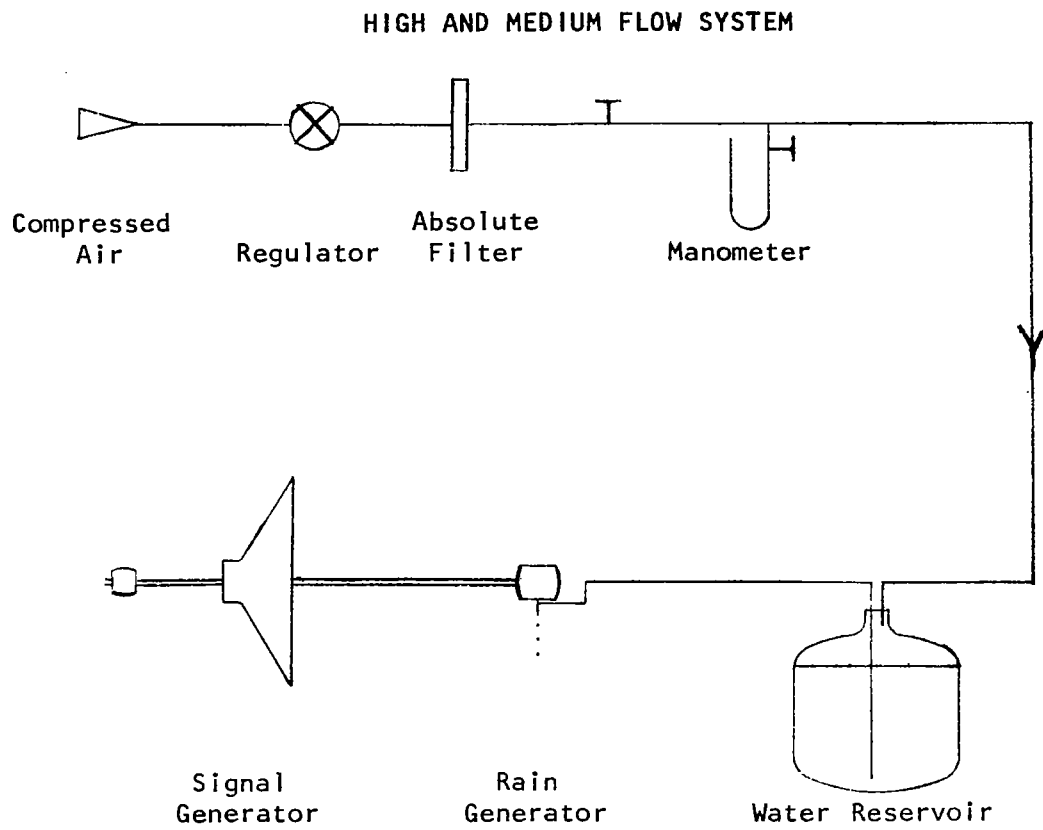


Figure 7
RAINDROP GENERATOR

water. The flow rate of the rain water was regulated with the use of carefully controlled compressed air. The complete generation system was located outside the experimental chamber to facilitate changing droplet size during scavenging tests.

Three raindrop sizes were generated during the performance of the scavenging experiments. These sizes were 0.55mm, 1.1mm, and 3.0mm in diameter and covered the operating range of the generation system used. Operational data for each of the raindrop sizes tested are given in Table 1.

Preliminary experiments were conducted with the raindrop generation system to evaluate overall performance. The generator was set-up in the laboratory under the desired experimental conditions and the generated droplets were photographed using a special optical system. A linear scale was located adjacent to the falling droplets to directly determine size.

The 3.0mm drops were found to be too close together (~ 0.5 mm gap) for adequate mixing with the rocket exhaust cloud. As a consequence, a 18mm separation was achieved with a reduced - Table 1 - liquid flow rate. Rayleigh break-up of the liquid jet was clearly observed at the new flow condition and, therefore, ensured uniformly sized droplets. However, the droplet terminal velocity was not achieved at the exit of the hypodermic tube. A corrected time interval or residence time for the 3.0mm droplet within the experimental chamber was measured and used to correct the HCl scavenging data. The actual residence time was based on 16mm movie camera photographs of the falling drops inside the experimental chamber. The camera was operated at a speed of 32 frames-per-second using Tri-X (Kodak) film. Through the use of special lighting techniques, the raindrops were observed to produce visible tracks on the film. The number of frames counted for the complete fall of the drops varied from 22 to 26. This gave an average residence time of 0.75 sec. for the 3.0mm droplets. The calculation of the HCl scavenging rates incorporated this pre-determined residence time.

The 1.1mm droplets were spaced approximately 2.5mm apart and as determined from the photographs, were uniformly sized and

Table 1

RAINDROP GENERATION SYSTEM CHARACTERISTICS

<u>raindrop Size (mm)</u>	<u>Liquid Jet Diameter (mm)</u>	<u>Needle Gage (Regular Wall)</u>	<u>Settling* Velocity (cm/sec)</u>	<u>Liquid Flow Rate (cm³/min)</u>	<u>Excitation Frequency (HZ)</u>
0.55	0.292	24	225	9.0	1705
1.1	0.584	20	434	69.8	1648
3.0	1.60	14	806(72.9)	88	101

Based on work by Gunn and Kinzer (11). Velocity in parentheses is the actual droplet velocity upon droplet formation.

falling at their terminal velocity. The droplet size measured with the use of the scale was 1.1mm.

The generation of the smallest droplets was initially expected to occur in the 0.3mm range, but practical limitations necessitated an increase in droplet size to 0.55mm. Due to the dominating influence of the liquid's surface tension and imperfections at the nozzle tip severely deflecting the liquid jet, 0.3mm drops could not be reliably generated. Preliminary experimentation determined that 0.55mm droplets avoided these problems and could be generated at their terminal fall velocity. Separation distance between adjacent falling droplets was approximately 1mm.

A commercially available fog nozzle* was secured and set-up near the experimental chamber. The fog nozzle had a liquid rate of 0.076ℓ/min and required both a fixed gas pressure of 60 psig and a variable liquid supply pressure of 5-30 psig. Stainless steel was used in the construction of the nozzle. The advertised droplet diameter was from 10 to 5 μm. The actual size of the droplets was measured to be an average of 10 μm (based on number). Visual appearance of the fog definitely suggested strong similarity with naturally occurring fog. Time required to fill the experimental chamber with a "thick" fog was on the order of 15 seconds -- waiting time was minimized. The fog nozzle itself was kept outside the experimental chamber at all times except when fog was introduced into the chamber. At this point, the nozzle was inserted through the open door of the experimental chamber, permitting the fog to flow into the Teflon bag. A Millipore filter was used in the water line of the fog nozzle to prevent clogging.

2.4 Rain Collection

The rain collection system was located at the bottom of the experimental chamber. The design of the collection system was to prevent the "collected" raindrops from contacting the HCl exhaust cloud above. This was crucial because the separate application

*Heat Systems-Ultrasonics, Model 700; New York, New York.

of a blank was avoided and the collected rain sample could be analyzed directly.

Final design of the rain collection system is given in the schematic diagram of Figure 8. A 20 cm (8 in.) diameter pyrex funnel was used to direct the collected raindrops to a holding flask. All fittings were ground-glass to minimize HCl losses. Nitrogen was introduced into the flask and flowed upward forming a natural barrier to the HCl cloud above: Exit ports were located along the periphery of the funnel to remove the nitrogen. The flow through the periphery ports was adjusted to match the flow rate of the incoming nitrogen (14.2 lpm). The sheath formed by the nitrogen trapped the exhaust cloud within the experimental chamber while maintaining the cloud's natural concentration and decay rate. The funnel assembly was sealed at the bottom of the chamber by a soft rubber gasket which facilitated removal from its holder for cleaning between scavenging experiments.

A blank of the rain water was obtained during each series of scavenging experiments. The blank served as a correction to the initial Cl^- content of the rain water and was generally found to be relatively low. Analysis for the Cl^- content of the rain droplets employed a chloride-specific ion electrode for the first 3 rockets ignited and colorimetric determination for the last two rocket tests.

2.5 Measurement of Hydrogen Chloride Concentration

The measurement of the rocket exhaust cloud HCl concentration is important and has direct input to the raindrop scavenging data. A meeting was held at NASA-Langley to determine the most suitable detection method for HCl within the experimental chamber. The people contacted at NASA-Langley were Dr. Gerry Gregory and Dr. Scott Wagner of the Atmospheric Environments Branch. Agreed at the meeting was the overall suitability of the chemiluminescent HCl detector (Geomet)* for use in the IITRI experimental program.

*Geomet, Incorporated, 2814-A Metropolitan Place, Pomona, Calif.

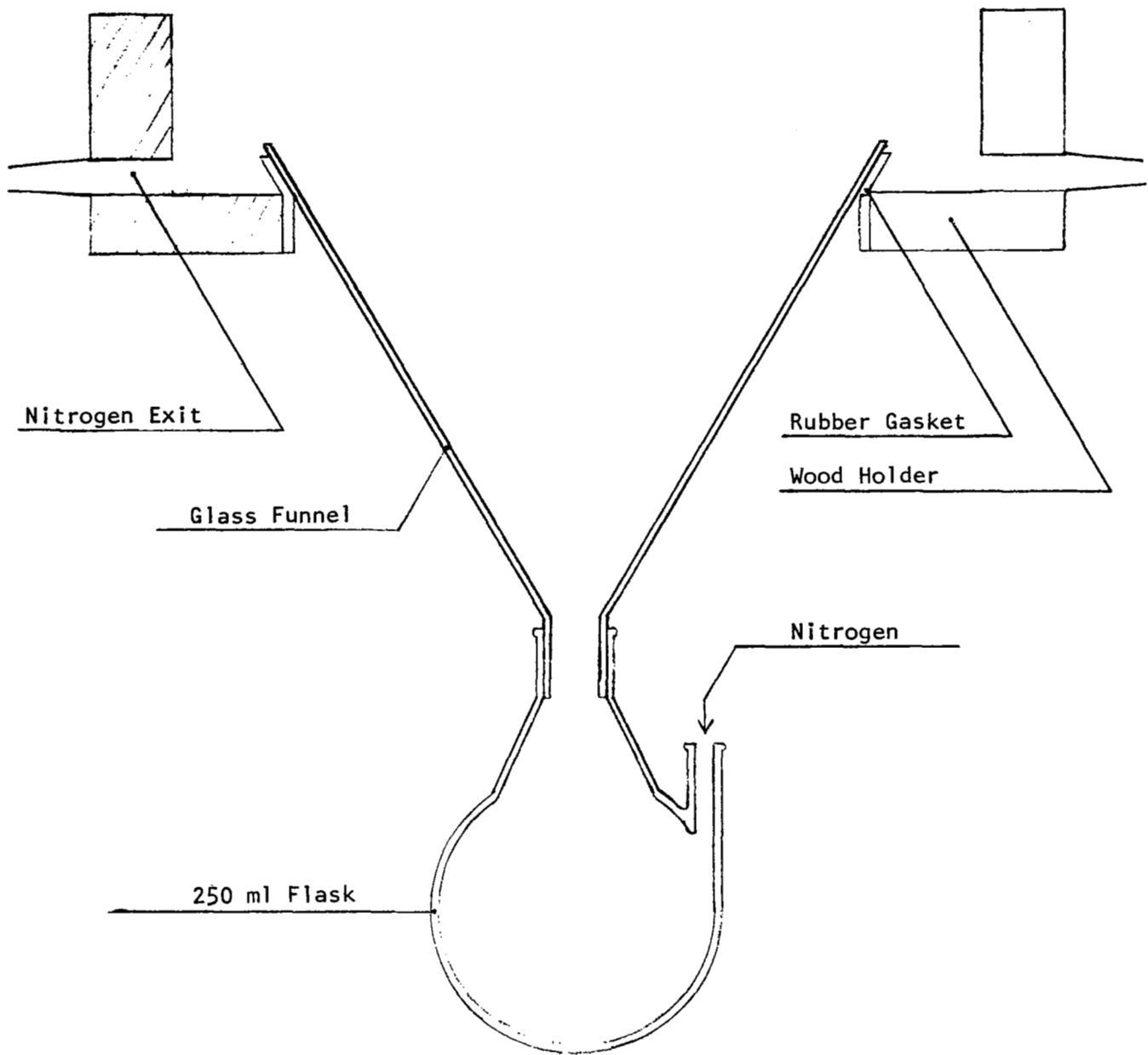


Figure 8
RAINDROP RECEPTACLE

NASA-Langley, at the early phase of the IITRI program, had experienced some difficulty with the gaseous phase HCl calibration procedure. The difficulty was in the passivation of the system to the low HCl concentration levels--about 1 ppm. For this reason, a liquid calibration procedure was recommended to IITRI.

Two Geomet HCl detectors were acquired for use during the program. The first instrument was purchased outright by IITRI and the second was borrowed over the program's length from NASA-Langley. First, the instruments were calibrated--both at the initiation and conclusion of the scavenging tests to determine and quantify sensitivity drift. Second, a technique was developed and experimentally evaluated permitting the physical separation of the gaseous and liquid phase HCl. The performance of the Geomet detector has already been documented by NASA-Langley, but careful calibration was nevertheless required.

The NASA-Langley "Field Calibration Procedures for Chemiluminescent Hydrogen Chloride Detector" was used in the calibration effort at IITRI. The resultant instrument accuracy as a result of this method of calibration was approximately ± 15 percent. The procedure called for the injection of a solution of known HCl concentration. The detector's response was then measured and related to the amount of HCl injected. Because the HCl was in a liquid solution, a syringe was used to inject the liquid into the instrument's sample inlet tube. The composition of the HCl calibration solution is given below:

1. 4.9 ml methanol
2. 0.1 ml H₂O
3. 25 μ l constant boiling HCl azeotrope

The above fluid contained about 5.5×10^{-6} gm of HCl per 5 μ l of solution.

The scale factor calibration--electronic gains between output scales on the instrument--were checked and found to be very near the nominal values (see Table 2) throughout the duration of the program. The sample flow rates were also checked and set at 2.0 lpm. Modification of the IITRI detector was necessary to

Table 2
SCALE FACTOR CALIBRATION FOR THE
HCI DETECTORS

<u>JITRI Detector</u>	<u>Langley Detector</u>
$SF_1^* = 9.94$	$SF_1 = 10.14$
$SF_2^{**} = 9.93$	$SF_2 = 10.00$
$SF_3^{***} = 9.99$	$SF_3 = 10.04$

* SF_1 -- scale factor for X1 and X10 scales.

** SF_2 -- scale factor for X10 and X100 scales.

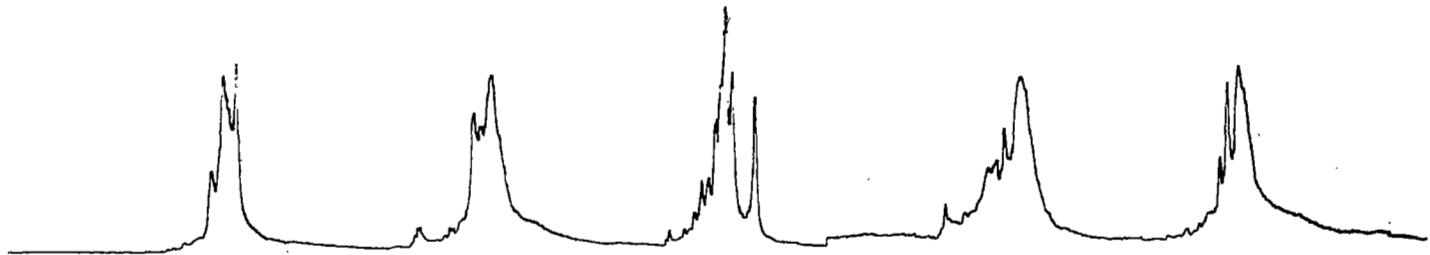
*** SF_3 -- scale factor for X100 and X1K scales.

achieve the desired 2.0 lpm. Also, the inlet tube was recoated frequently to insure no depletion during calibration.

Liquid injections were made at the 3 μ l level to constrain the instrument response within the range of the recorder. Figures 9 and 10 show the typical traces obtained. The area under each response was calculated through the use of a Hewlett-Packard 9100B desk calculator and plotting board. At the beginning of the program, the IITRI detector exhibited a sensitivity of 10.85 ppm/volt on the X1 scale while the Langley instrument gave 12.51 ppm/volt. This was considered to be typical of instrument-to-instrument variation. At the conclusion of the test program, the borrowed NASA-Langley detector had a sensitivity of 17.1 ppm/volt on the X1 scale while the IITRI purchased detector had a 19.3 ppm/volt sensitivity on the X1 scale. Application of the scale factor calibration yielded the sensitivity of the remaining scales. A significant shift in detector sensitivity occurred over the test sequence and, therefore, the data were corrected to compensate for this shift.

A separate auxiliary experiment was conducted concerning the detection of airborne HCl. During the first set of IITRI tests (12), bubblers, employing distilled water as the collection liquid, were used to measure the HCl concentration during the scavenging tests. Questions arose revolving around the reliability of the bubbler technique. To check on this question, two midget impingers were connected in series, filled with 50 ml of distilled water each, and used to sample the experimental chamber's contents. When the chamber concentration was approximately 1.8 ppm HCl (1.82 ppm time-weighted-average), the bubbler train, operated at 4.9 lpm, indicated 2.0 ppm HCl (13 min). The chemiluminescent HCl detector was taken to give the true HCl concentration and the associated percentage error was calculated as 10%. This was considered reasonable in view of the low HCl concentration and gave credence to the earlier IITRI scavenging results conducted at significantly higher HCl concentrations.

Chart Speed = 1 mm/sec (→)
2 cm/volt
HCl IITRI Detector



24

Figure 9
LIQUID CALIBRATION RESPONSE FOR THE IITRI HCl DETECTOR

Chart Speed = 1 mm/sec (→)
2 cm/volt
Langley HCl Detector

25

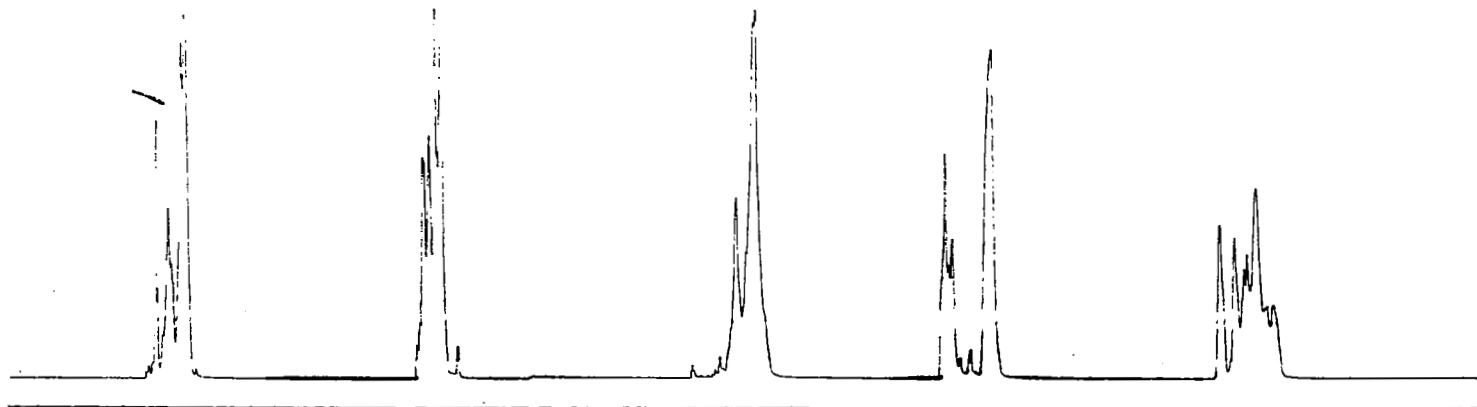


Figure 10

LIQUID CALIBRATION RESPONSE FOR THE LANGLEY HCl DETECTOR

Depending on the "local" relative humidity, the combustion generated HCl might be in the gaseous phase or in both the liquid and gaseous phases. This aspect had significant consequences relating to the washout (below raincloud) of HCl. If a portion of the HCl was contained within the liquid phase, the washout rate was reduced because of the lowered collision efficiency of raindrops with the smaller droplets. However, during the initial washout experiments conducted at IITRI, the expected large reduction did not occur under the predicted circumstances. Therefore, improved experimental techniques were developed to provide details of the HCl gaseous/liquid partition.

Several experimental schemes were explored, but only one held promise. Before describing the technique utilized, the others should be mentioned. Precipitating the liquid HCl droplets by means of an applied electrical field was considered because collection efficiencies are good for submicron droplets (impaction is not adequate for submicron droplets). However, an electrical precipitator was attempted by Dawbarn (13) and failed to function properly. An additional problem was the likely liberation of the once liquid-borne HCl, thus providing an error in the measurement of gaseous HCl. It appeared that this re-liberation phenomenon could not be overcome. The same was true for direct filtration; once the droplets were collected, they would evaporate due to the passage of unsaturated air. No fool-proof scheme could be devised to fix the HCl (liquid phase) to the filter substrate.

Whereas both of the above approaches removed the liquid phase from the gaseous phase, it was also possible to trap the gaseous phase HCl while allowing passage of the HCl droplets. Capillary tubes in a parallel configuration were found to provide adequate opportunity for gaseous diffusion of HCl to the walls, thus passing the liquid phase droplets. The material used to construct the capillary tubes must fix the HCl once contact was made. Due to HCl's high chemical activity, a suitable surface

was not difficult to locate--in fact, copper, brass, or stainless steel tubing were all candidates.

With the capillary tubes, the gaseous HCl was lost and the liquid phase HCl was introduced into the detector. A second HCl detector measuring total HCl then provided sufficient detail to determine the partition of the gaseous and liquid phase HCl. Subtracting the total HCl concentration from the liquid phase HCl concentration gave the gaseous phase HCl concentration.

Calculations have been performed to determine the performance obtainable in fixing the gaseous HCl by means of capillary tubes. Sherwood, et. al. (14) gives the following relation yielding the concentration of a gaseous species as a function of axial length along the tube.

$$\frac{C_i - \bar{C}}{C_i - C_o} = 0.819e^{-14.63\beta} + 0.0976e^{-89.22\beta} + \dots,$$

where

$$\beta = \frac{x}{4r_o^2 \bar{U}}$$

C_i = initial gaseous concentration

C_o = final gaseous concentration

\bar{C} = average gaseous concentration

= diffusion coefficient

x = axial length along tube

r_o = tube radius

\bar{U} = mean flow velocity inside tube.

The results of an example calculation are given in Figure 11 showing the decrease in gaseous phase HCl concentration with downstream distance. The left-hand side of the above equation can be referred to as the relative penetration. The calculation assumes specific operating conditions that have been manipulated to give good performance yet maintain simplicity of construction.

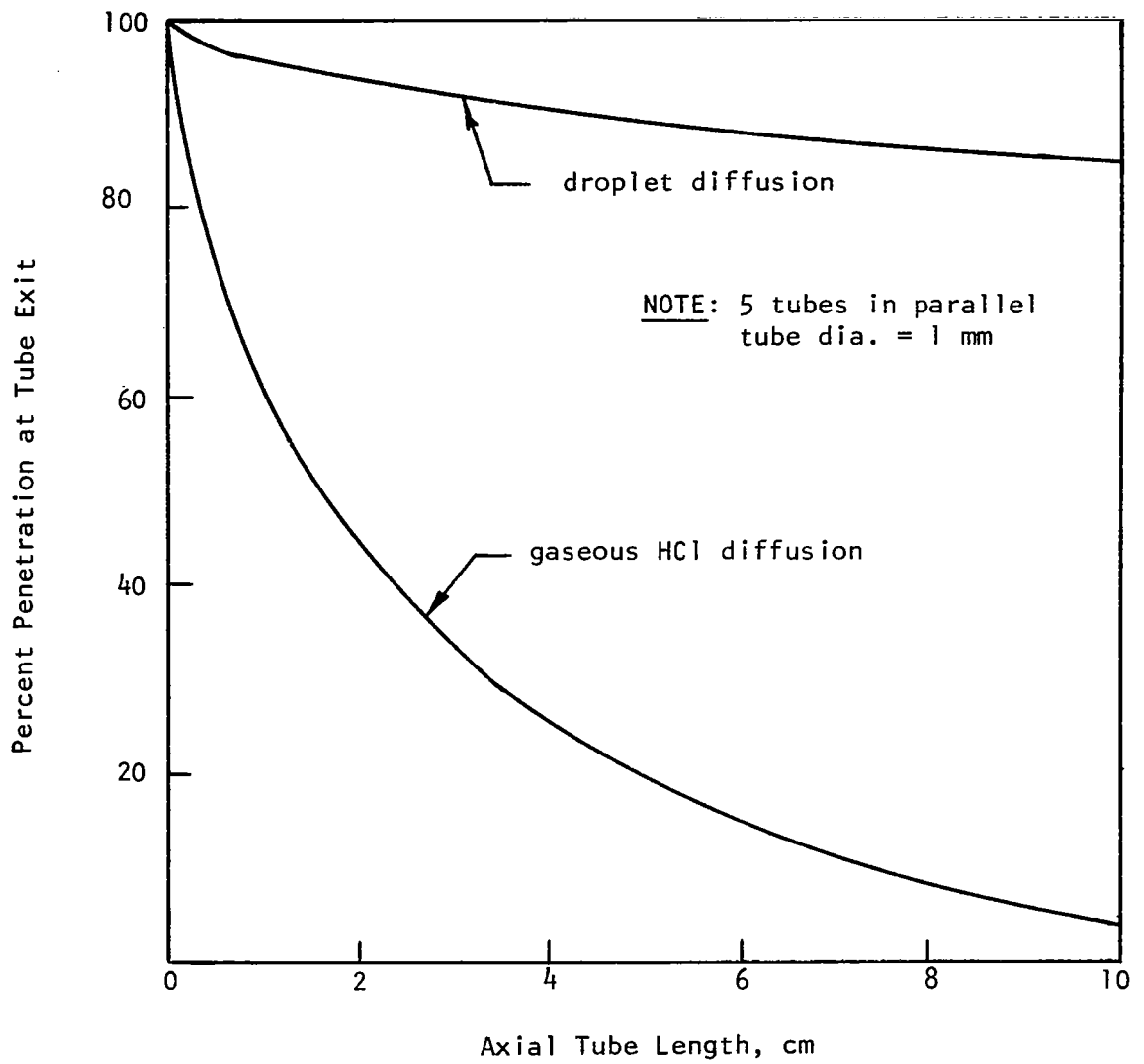


Figure 11
CALCULATION RESULTS FOR DROPLET AND GASEOUS DIFFUSION OF
HCl SHOWING THEORETICAL MAGNITUDE OF SEPARATION

The tube diameter was 0.10 cm and the bundle consisted of 4 copper tubes. Because the sample flow rate into the HCl detector was 2 lpm, the velocity within the tube was not arbitrary, but 843 cm/sec. Calculations for the losses of droplets to the wall require knowledge of size. Fuchs (15) gives for steady laminar flow

$$\frac{\bar{n}}{n_i} = 0.891e^{-3.657\alpha} + 0.097e^{-22.3\alpha} + 0.032e^{-57\alpha} + \dots$$

where

$$\alpha = \frac{D' x}{r_o^2 \bar{U}}$$

and D' is the diffusion coefficient for the droplets, \bar{n} , the mean number concentration of the droplets, and n_i the initial number concentration of the droplets. The influence of droplet size is made through D' , which varies inversely with size. If a droplet diameter of 2 μm is selected, the curve on Figure 11 is obtained giving the relative number of droplets (penetration) surviving the capillary tube. Larger droplets give greater survival while smaller droplets give less. Gillespie and Johnstone (16) obtained droplets grown in the presence of HCl gas to mean sizes of 5.5 μm while the IITRI work on the HCl-H₂O vapor systems yielded droplets of approximately 0.7 μm growing rapidly to larger sizes in a dynamic system (17). Since the exhaust material within the test chamber was contained for a reasonable time interval, the droplets grew providing the local conditions were correct (sufficient relative humidity).

To evaluate the workability of the diffusion battery concept, a preliminary laboratory experiment was conducted. A special air dilution system was constructed as shown in Figure 12. The purpose of the dilution system was to deliver gaseous HCl at a pre-determined concentration based on precise air dilution flow rates. The method depended on knowing the initial concentration of the HCl prior to dilution.

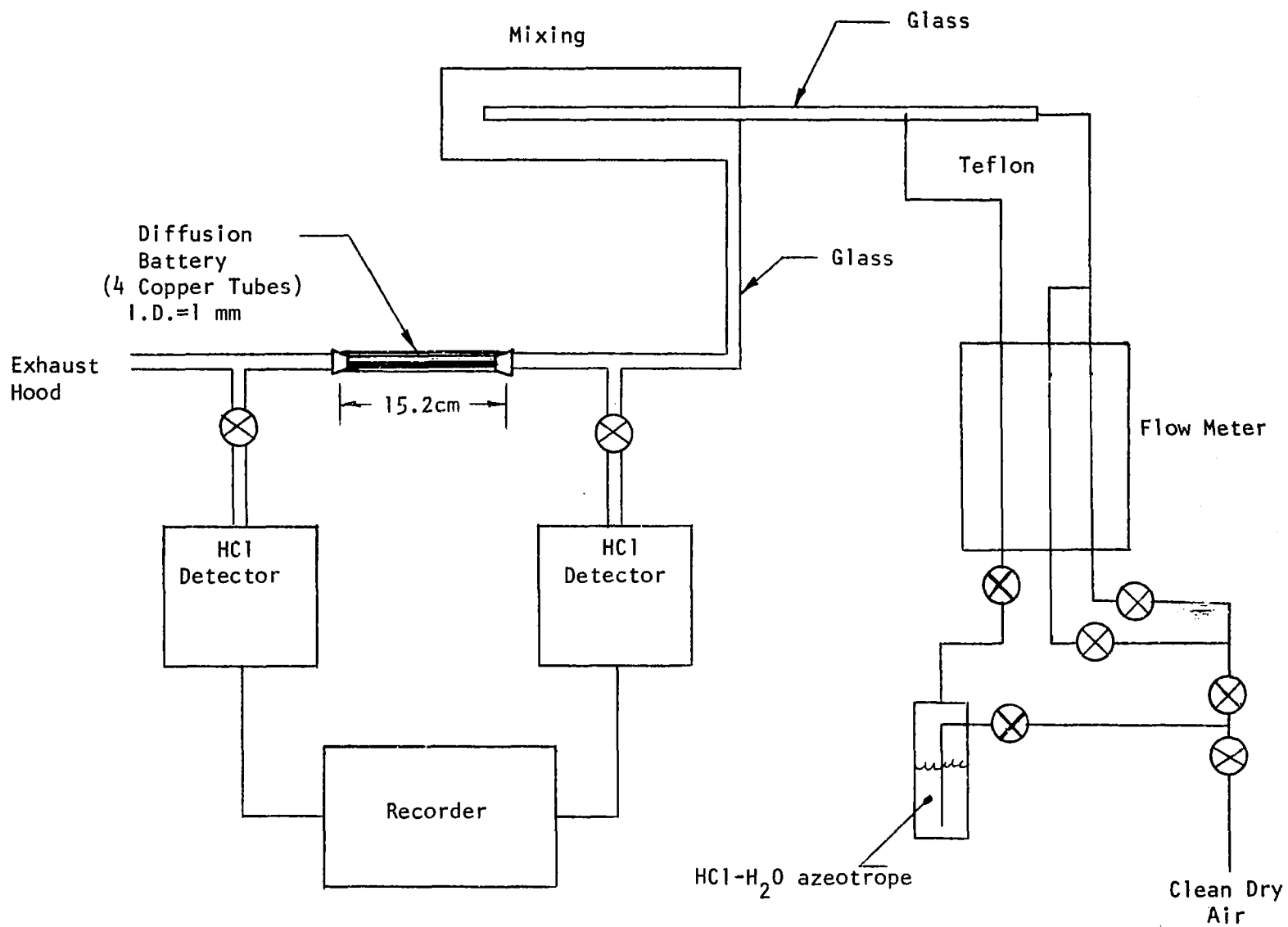


Figure 12

SCHEMATIC DIAGRAM OF AIR-DILUTION SYSTEM

A commercial high pressure tank of HCl gas diluted with nitrogen to 998 ppm HCl (certified) was purchased to provide the known source of HCl. However, when the total dilution system was operational, the HCl content was drastically reduced as indicated by the Geomet detectors. Humid air was introduced to the dilution air with no change in HCl response. Therefore, it was concluded that the HCl in the tank had probably reacted with the metallic walls. As indicated in Figure 12, the HCl bottle (tank) was replaced with the HCl-H₂O azeotrope.

A larger flow rate (8 lpm) was passed through the diffusion battery (15.2 cm long). Carrying out the calculations based on gaseous diffusion mechanisms, the HCl concentration ratio was 0.39 while the measured ratio was 0.5. This ratio remained constant for approximately an hour indicating the expected "life" of the copper tubes. Concluded, therefore, was the workability of the copper diffusion battery concept for the separation of the gaseous and liquid phases of HCl.

2.6 Absorption Chamber

The absorption of HCl by terrestrial surfaces such as sea water and the ground could significantly affect the HCl concentration predicted by the MSFC multi-layer diffusion model. The MSFC model, at the present stage, assumes no absorption at the surface but can be easily modified to account for HCl loss by a normalized "absorption" coefficient.

During the absorption chamber experiments, four surfaces were evaluated for relative HCl uptake. The surfaces tested included distilled water, sea water, brackish water, and a reference solution of NaOH (0.05 Normal). The reference solution serves as the normalization surface for the HCl uptake. The composition of sea water was privately obtained from Mr. Chao Schem at the Naval Air Propulsion Test Center (18) and is given in Table 3.

The composition of brackish water cannot be precisely specified. In fact, the term "brackish" is very general and incor-

Table 3
COMPOSITION OF LABORATORY SEA WATER (18)

<u>Sea Water:</u> 1 liter	
NaCl	23 g
NaSO ₄ • 10H ₂ O	8 g
stock solution	20 ml
distilled water	to yield 1 liter
 <u>Stock Solution:</u> 1 liter	
KCl	10 g
KBr	45 g
MgCl ₂ • 6H ₂ O	550 g
CaCl ₂ • 6H ₂ O	110 g
distilled water	to yield 1 liter

porates the marshy backwater of rivers, the bay areas near the sea, and industrial effluents. Consequently, the brackish water most desirable for these absorption experiments is that water from the Cape Kennedy area. However, our experiments were not of sufficient precision to warrant the expense of obtaining specific brackish water. A "working" definition of brackish water was obtained from the Environmental Protection Agency (Region 5) and was applied here--40% solution of sea water with distilled water.

The normal procedure for calculating the removal rates of gaseous pollutants involves the so-called deposition velocity. The deposition velocity is defined by

$$F = V_g c$$

where F is the downward flux of the gas and c the concentration of the gas at a specified height above the surface where the deposition occurs. Another approach utilizing the concentration gradient immediately above the surface and the local atmospheric diffusivity can also be used to determine deposition velocity but was unsuitable for the present experimental facility. Measurement of the turbulent diffusivity would be much too cumbersome. Therefore, V_g was determined as given in the above simplified equation.

The use of deposition velocities rather than total fluxes was desirable because the data are automatically corrected for differences in HCl concentration. The experimental data obtained gave the HCl flux, F , and an average HCl concentration measured downstream from the absorbing surface. Concentration values were also checked upstream and were found only slightly higher than the downstream values.

Figure 1 shows the general location of the absorption duct within the overall experimental facility. The rocket exhaust cloud must pass through the duct assembly upon transport to the experimental chamber. The dilution system, with its ability to

provide excess air at varying humidity, served to regulate the volume flow of rocket exhaust from the spherical holding chamber.

The design of the HCl absorption duct is given in Figure 13. Galvanized steel sheet was used to form the walls of the duct. The inside surface was coated with an epoxy-resin paint to minimize HCl loss and subsequent corrosion of the inside surface. Two and one-half cm (1 in.) pipe fittings comprised both ends of the duct and facilitated connection to the remainder of the experimental system. The transition from the 15 x 10 cm (6" x 4") rectangular duct to the one inch pipe fittings was 15 cm (6 in.) long and rectangular in cross-section. The total length of the straight portion of the duct was 60 cm (2 ft.). A tray was provided for the absorption experiments which was 5 cm by 30 cm (2" x 12") and approximately 2.5 cm (1 in.) deep. A gasket was used to provide a tight seal between the 2.5 cm (1 in.) flange on the tray and the bottom of the duct.

Basically, the experimental procedure was to measure the HCl picked-up by various surfaces through analysis of the surfaces themselves for chlorine. Knowing the HCl concentration, velocity, and exposure time would yield the "absorption rate", deposition velocity, and the mass transfer coefficient. The term "absorption rate" is not precisely correct because absorption is a specific local mechanism and separate from HCl transport to the surface where absorption may or may not occur.

A question arose regarding the fact that the experimental procedure did not measure the actual depletion (or depletion rate) of the passing HCl exhaust flow. Therefore, the suggested experimental plan was to measure both the inlet and outlet HCl concentration and by arithmetic difference, calculate the rate of HCl depletion. An initial inlet and outlet measurement was required with the absorption chamber empty in order to "calibrate" the wall losses. Therefore, the difference between the calibration test and those with various absorbing materials gave the depletion rate of HCl for the specific materials exposed

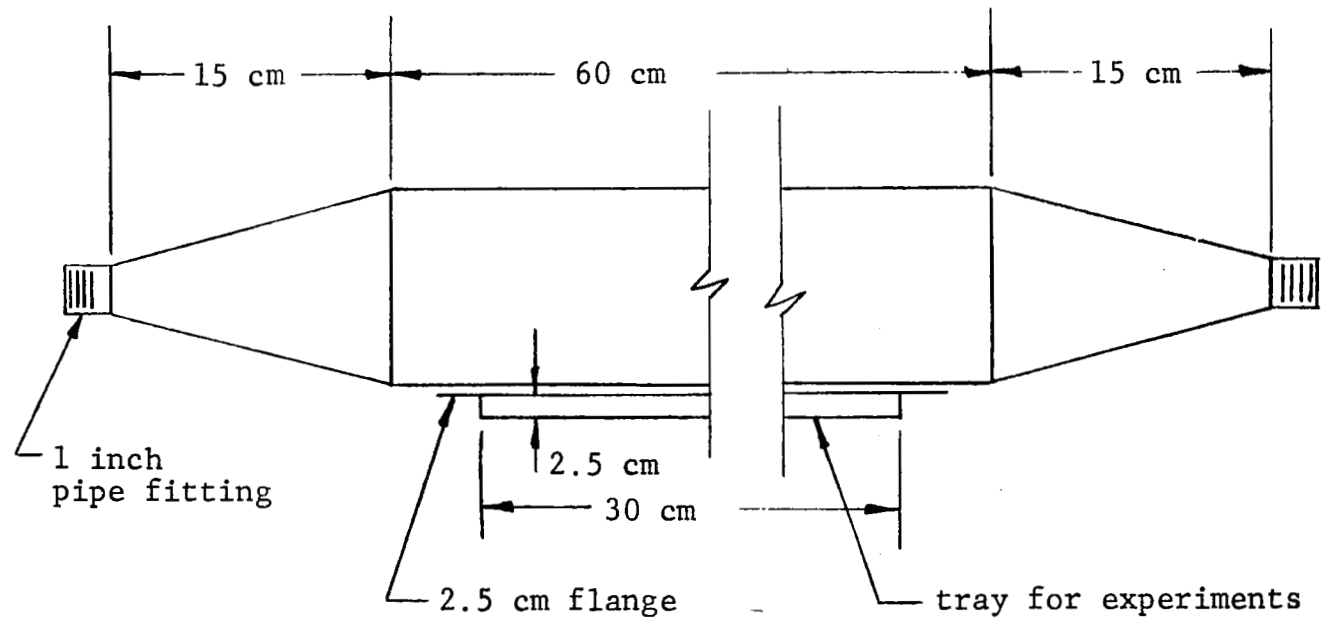


Figure 13

DESIGN OF DUCT FOR HCl ABSORPTION EXPERIMENTS

- Note: 1. Duct cross-section is 15 cm x 10 cm.
2. Tray inside dimensions is 30 cm x 5 cm x 2.5 cm deep.

To check the workability of the suggested procedure, a preliminary experiment was conducted. Figure 14 shows a schematic diagram of the test equipment. The absorption chamber used was the same as constructed for the HCl absorption experiments. A supply of clean air (regulated and filtered) was passed through an HCl-H₂O azeotrope to deliver gaseous HCl. Shop air, monitored with an inclined manometer, provided the main air flow through the absorption chamber. A dry-test meter was used to measure total flow rate and calibrate the flow system.

Table 4 gives the results obtained for both the chamber calibration runs and the distilled water test runs. All the tests were conducted in the HCl concentration range of ~ 1 ppm. Noted immediately was the consistent reduction of the HCl concentration upon passage through the chamber. However, an explanation cannot be offered as to why the distilled water tests yielded a lower HCl concentration difference than the empty chamber tests. The difference should have been greater due to the presence of the distilled water (HCl sink). Consequently, the reliability of the HCl concentration measurement may be suspect. The calibration error in the HCl detectors is in the vicinity of $\sim 15\%$ on the 10 ppm HCl scale (based on the calibration previously performed). Therefore, the uncertainty in the HCl measurement is about ± 1.5 ppm on this scale. The differences in HCl concentrations measured by the two HCl detectors are well within this uncertainty and are, therefore, not reliable. This does not mean that the HCl detectors are not suitable for general measurement of HCl concentration levels, but only that their application here was unwarranted due to the precision required.

Further, the distilled water was retrieved and analyzed for Cl⁻ content with the use of an ion-specific electrode. These results are also shown in Table 4 where a steady increase in Cl⁻ content of the distilled water is observed with increasing mean velocity within the chamber. Measurement of the Cl⁻ content of the distilled water was strictly routine. Thus, the determination of the HCl mass flux to the surface was readily available.

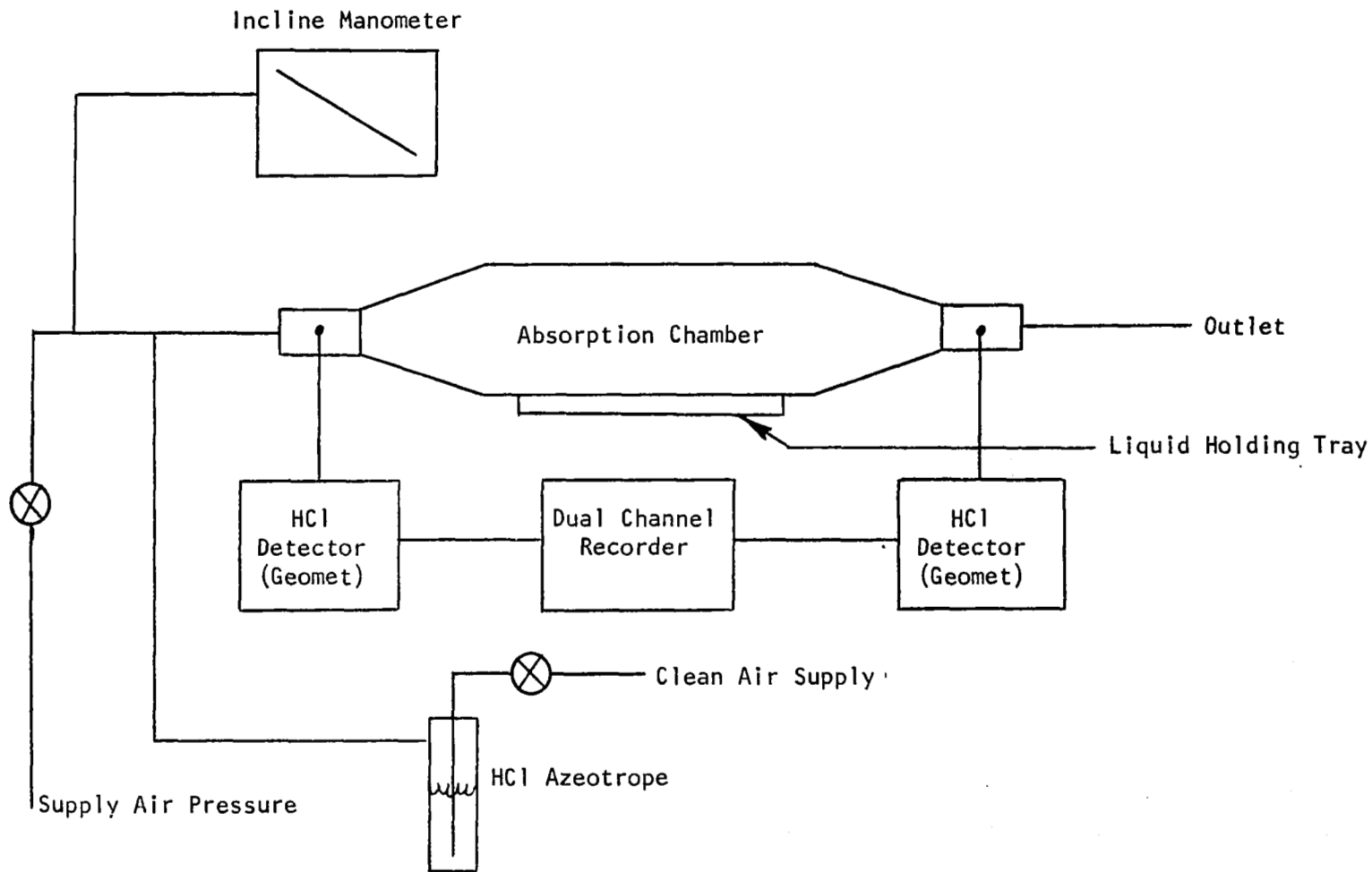


Figure 14

SCHEMATIC DIAGRAM OF EQUIPMENT USED IN PRELIMINARY HCl ABSORPTION EXPERIMENT

Table 4

PRELIMINARY TEST RESULTS FOR ABSORPTION CHAMBER

Chamber Calibration	<u>Time Interval min.</u>	<u>Mean Velocity (cm/sec)</u>	<u>Measured Total Cl⁻ Content** (mg)</u>	<u>Inlet HCl Conc. (ppm)</u>	<u>Outlet HCl Conc. (ppm)</u>	<u>HCl Conc. difference</u>
	(stable)	3.97	-	0.98	0.545	0.44
	(stable)	5.21	-	1.23	0.76	0.47
	(stable)	7.30	-	1.48	1.10	0.38
Chamber Test with Distilled Water						
	10.8	3.97	0.32	0.98	0.82	0.16
	9.2	5.21	0.54	1.35	1.20	0.15
33	9.9	7.30	1.1	1.35	1.31	0.04

* Based on cross-sectional area of absorption chamber

**Total volume of distilled water \cong 200 ml, distilled water -- 0.22 mg Cl⁻

Figure 15 displays the three data points in terms of the mean HCl fluxes through the absorption chamber and into the distilled water.

As a consequence of this preliminary absorption duct experiment, the employed methodology of HCl detection was not suitable for absorption rate measurements based on differences. The required accuracy and precision of measurement was beyond the instrument's calibration errors. Therefore, the direct measure of Cl^- within the absorbing media was performed for each of the uptake tests.

2.7 Growth Chamber for Experimental Plants

Selection of the plant material to undergo HCl uptake experiments was made at the beginning of the program. Before representative samples of the flora in the area of the Shuttle launch site are monitored, experimental plants serving as standard laboratory subjects, where background Cl^- measurements have already been performed under numerous conditions, should be evaluated. This was the approach taken with the experimental program conducted here.

The two standard representative plant material types are:

- monocotyledonous plants (oats and corn)
- dicotyledonous plants (peas and beans)

The actual plants selected were corn and soybeans for the practical reasons of easy growth and care.

A "growth chamber" was built to enable controlled plant growth. This chamber permitted control of the humidity, temperature and light that the plants received, thus removing some of the variables normally present. The growth chamber (Figure 16) consisted of the growing area approximately 2.43m x 1.83m x 1.23m (8' x 6' x 4'), a humidifier, blower, heater, and light tray. The light tray had twelve F96T12 high-output fluorescent tubes and six 150w/130v incandescent lamps to simulate the light spectrum produced by the sun. For optimum growth the plants require about 2000 ft-candles of light. To allow for growth, the height of the light tray was adjusted to maintain the 2000 ft-candles intensity.

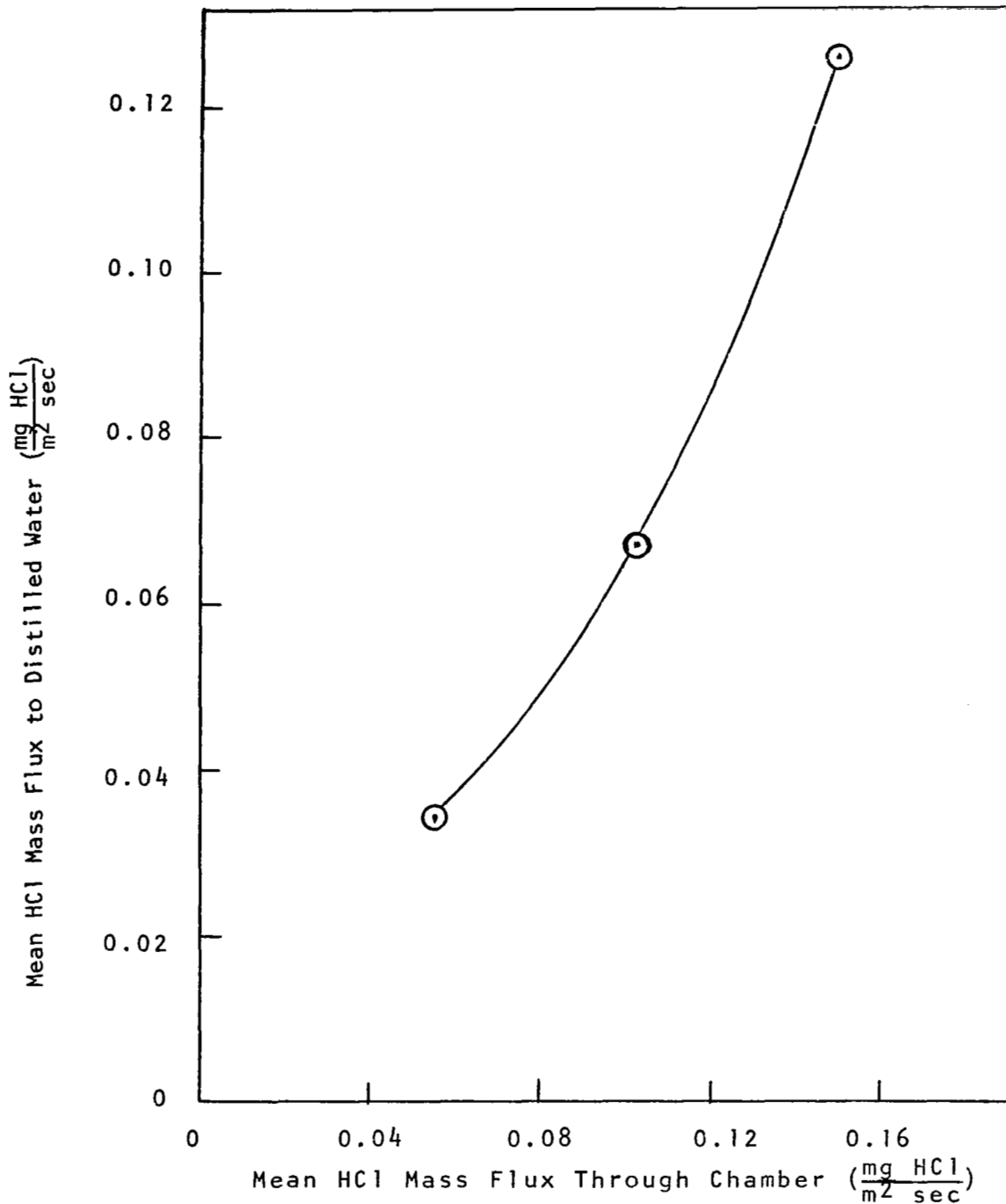
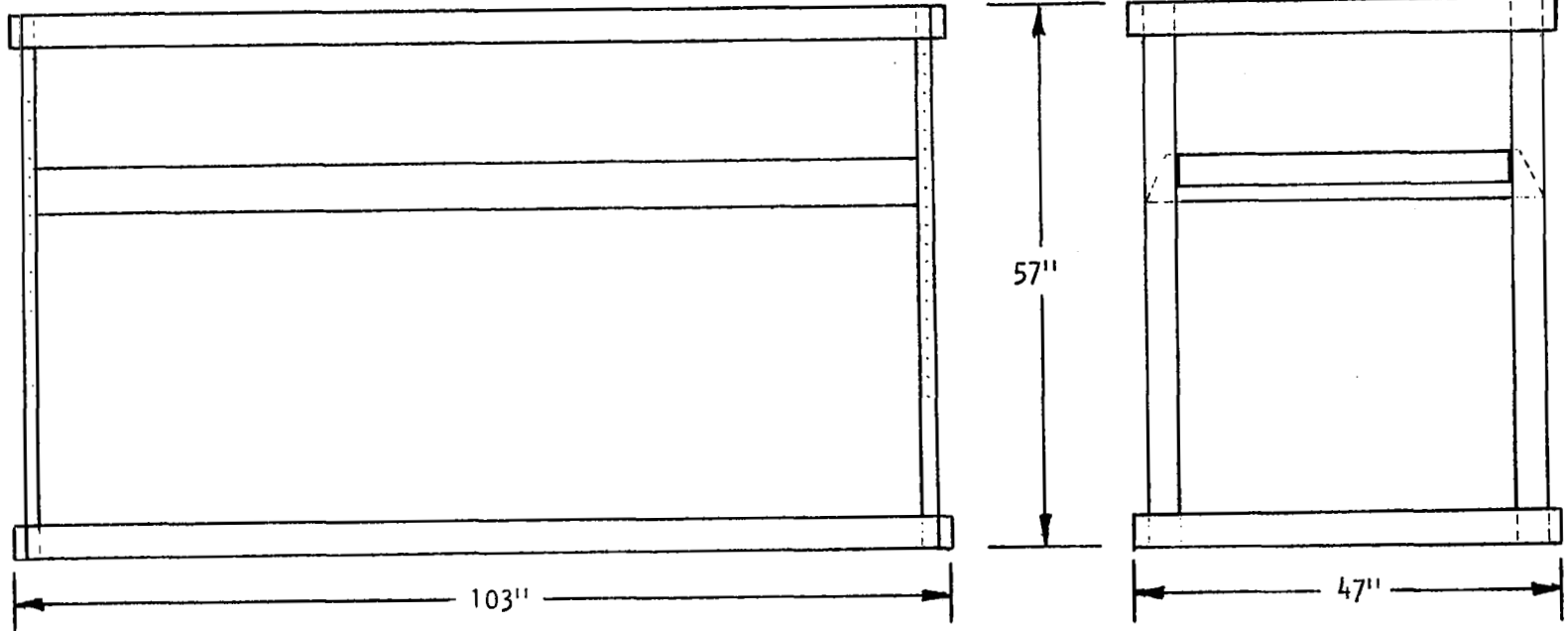


Figure 15

SURFACE ABSORPTION FLUX OF HCL TO DISTILLED WATER VERSUS MEAN GASEOUS HCL FLUX ABOVE SURFACE

Greenhouse



Light Tray

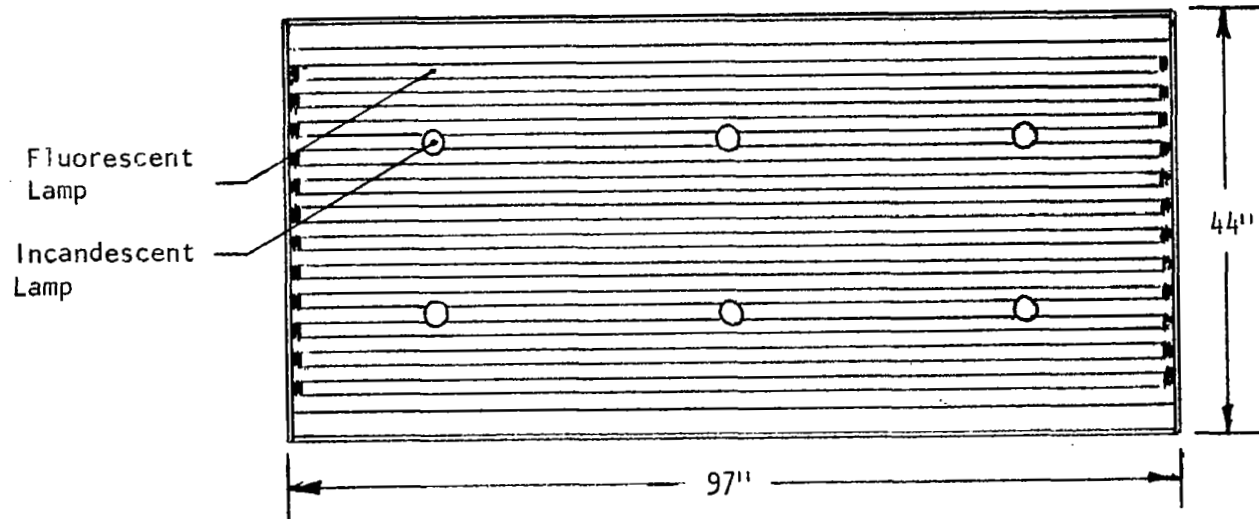


Figure 16
PLANT GROWING CHAMBER

The photograph shown in Figure 17 was taken about 3 weeks after planting the seeds. Both corn and beans were raised - the beans are behind the corn and are only partially visible. The growth achieved demonstrates the growing capacity of the chamber.

The plant watering system was made automatic. Tygon tubing along the upper edge of the plant box had small holes that produced small jets of water when the line was pressurized. The jets possessed sufficient strength to penetrate all the plants. A time interval of 15 seconds was found to keep the soil in a moist state. Timers were used to regulate the time of plant watering (only morning), the duration of watering, and the time period of lighting (12 hrs.). This was considered necessary to minimize the growing variations from one set of plants to another. Also, an adequate supply of seed was obtained to insure that all the seeds originated from the same source. The large conduits in the foreground of Figure 16 were the inlet ducts to the growth chamber from the humidifier providing cool mist air.

Preliminary experiments were carried-out to ascertain the number of plants needed to give a measurable chloride-ion background count. When using corn only 5 plants were required, but with soybeans 15 plants were necessary. The chloride-ion quantity at those numbers was easily measured by the chloride-ion electrode method. The time of growth for a useable sample for exposure in the experimental chamber was approximately two weeks after planting. Homogenization of the plants before analysis was done with the plants dried. In this way the plants could be stored without loss or change of the chloride-ion content until the analysis for Cl^- was performed.

2.8 Metallic Coupons

The corrosion of structural surfaces at the Kennedy Space Center, as well as those associated with private individuals (i.e. automobiles and homes), due to the presence of HCl within the ground exhaust cloud, were evaluated through the use of metallic coupons. In addition to the normal corrosion effects,

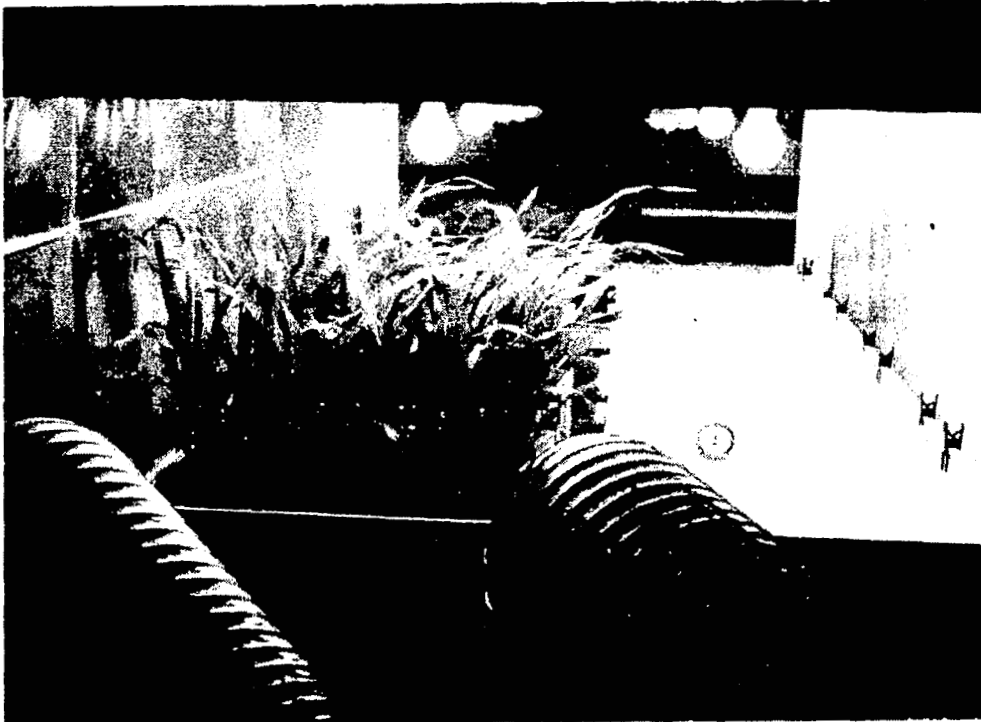


Figure 17

CORN AND SOYBEANS (BEHIND CORN) RESPONDING TO
CONDITIONS INSIDE GROWTH CHAMBER

premature failure of a structure might occur through stress-corrosion cracking. With stress-corrosion, any stressed metal or alloy could undergo failure at stresses below the normal fracture stress.

Test samples or coupons were fabricated from test alloys. Table 5 gives the alloy-types comprising the test matrix where each coupon was 2 inches square and 1/8 inch thick except for aluminum siding (building construction). The edges of each coupon were ground to a well-rounded profile to prevent any unusual or promoted corrosion in this region. In addition, stress corrosion specimens were fabricated from mild steel into a "U" shape with a bar welded across the open end of the "U". Mild steel was used for the painted coupons because automobile bodies and structural support systems are generally mild steel. One coupon was painted with a red lead paint while the second was painted with a typical automobile finish. A second austentic stainless steel coupon was coated with a special paint for space vehicles (S-13G). Therefore, a total of 9 test coupons comprised the matrix exposed to the rocket exhaust.

After exposure to the HCl rocket exhaust, the coupons were placed in a controlled oven maintained near saturated conditions. The temperature was constant at 95°F and a pan of water at the bottom of the oven maintained the high humidity. In this way, long-time exposures of the exposed matrices were possible. Weight differentials occurring from the exposure indicated the magnitude of the surface corrosion present.

3. EXPERIMENTAL PROCEDURE

The experimental procedure used during the tests is described here. Where required, clarification is provided after the specific procedure is identified.

1. Test chambers were prepared for rocket ignition. This included the sealing of the large spherical chamber to prevent loss of the rocket exhaust cloud. The experimental chamber was isolated (valve) from the contents of the large chamber. Experiments performed inside the large chamber were installed prior to sealing and rocket ignition.

Table 5
MATERIALS FOR CORROSION TEST MATRIX

Aluminum:	2024 6061
Steel:	mild steel
Austentic Stainless Steel:	304
Painted:	mild steel; red lead paint mild steel; automobile finish space paint
Aluminum siding:	coated

2. The rocket was ignited.
3. After approximately one minute had elapsed, the test plants and metallic coupons were installed within the experimental chamber. The rocket exhaust was drawn into the chamber until the desired concentration was achieved. The mixing fan was operated continuously to ensure uniform composition within the chamber. The decay in HCl concentration was compensated by adding more rocket exhaust as the exposure continued.

The exposure time was kept constant throughout all the tests at 20 minutes. This length of time is typical of the expected exposure time for the actual shuttle ground cloud. Lights were installed over the experimental chamber to maintain the test plants at the same conditions within the growth chamber.

4. Upon completion of the exposure period, the rocket exhaust was first purged from the experimental chamber. A record of the HCl concentration and relative humidity was obtained and the time-averaged values used to characterize the exposure (the fog nozzle was employed to increase the humidity when required). Retrieval of the plants and metallic coupons took place with the plants cut about 1 inch above the soil surface and dried immediately.
5. The rain scavenging tests were then performed. Again, with the application of the fog nozzle and alternate charging and bleeding of the experimental chamber, the desired test conditions were achieved. The raindrop generator was then started. During all the scavenging tests, the nitrogen flow to the rain collection system was operating. After a reasonable volume of raindrops was collected, the particular scavenging test was complete. The collected rain was removed and put in storage, the collection apparatus cleaned, and the rain generation system changed (excitation frequency, hypodermic needle, and liquid flow rate) before the next scavenging test was begun. All the scavenging tests were performed within this period of the test sequence.
6. The last series of tests involved the absorption duct assembly. The exit of the duct was monitored for HCl concentration. Valves were arranged in such a way to connect the absorption duct directly to the laboratory's negative pressure. In conducting a test, the lower tray was removed, cleaned, filled with the test liquid, and then re-installed. The rocket exhaust was then caused to flow through the chamber and diluted to give the desired HCl concentration. The exposure time period was on the order of 10 minutes. After the test was

complete, the tray was removed and the exposed liquid placed in storage for later analysis. Preparations were then made for the next test liquid.

7. At the conclusion of the test sequence, the large chamber was ventilated and the experimental chamber manually washed clean. Experiments conducted within the large chamber were now retrieved. Once ventilation was complete, the large chamber was washed-down with the internally located spray nozzle.

Once the chlorine analysis was completed and the test results reviewed, preparations were made for the next rocket firing.

4. EXPERIMENTAL TEST DATA AND RESULTS

4.1 Scavenging Test Results

The raindrop scavenging experiments were conducted over a wide range of HCl concentrations (0.2 to 10 ppm). Three raindrop sizes were selected to embrace the size range for naturally occurring rain. These raindrop sizes are 0.55mm, 1.1mm, and 3.0mm. Within this section of the report, the scavenging data is both presented and reduced to an empirical relationship.

4.1.1 Rocket Exhaust HCl Scavenging Data

The HCl scavenging data obtained with the experimental apparatus already described are given in Table 6. The relative humidity within the experimental chamber was determined for each scavenging test (battery operated dry-bulb and wet-bulb thermometer system). The variable, R_A , is the rate of HCl absorption by a single droplet of specific diameter and has the units--g/sec. The reported datum for the 0.3mm droplet is not considered reliable because difficulty was experienced with the rain-generating equipment. The remaining data, with the same experimental techniques and procedures applied to each, are considered reliable.

In reducing the experimental scavenging data, a parameter was sought to generalize all the data. A dimensionless-group of variables can be formed as $R_A/\rho V_s D_d^2$, where V_s is the terminal fall velocity for a particular droplet of diameter D_d . To force the units to cancel, the density of air, ρ , is introduced to the parameter. Plotting the parameter against the corrected HCl concentration (corrected for HCl detector drift), Figure 18 results.

Table 6

DROPLET SCAVENGING RESULTS FOR ROCKET EXHAUST HCl

Rocket Number	Size (mm)	Vol. (ml)	Total Cl ⁻ (μg)	Uncorrected Raindrop Cl ⁻ Conc. (μg/ml)	Reference Raindrop Cl ⁻ Conc. (μg/ml)	Corrected Raindrop Cl ⁻ Conc. (μg/ml)	Corrected HCl Conc. (ppm)	Experimental Chamber R.H. (%)	R _A (g/sec)
1	0.3*	14	600	42.8	10.9	31.9	7.0	~55	3.8 x 10 ⁻⁹
	1.1	152	4080	26.9	10.9	16.0	7.4	~55	3.5 x 10 ⁻⁸
	3.0	152	3000	19.7	10.9	8.8	8.0	~55	1.8 x 10 ⁻⁷
2	0.55	50	220	4.4	3.0	1.4	1.7	76	2.4 x 10 ⁻⁷
	0.55	44	1000	22.7	3.0	19.7	8.4	62	3.6 x 10 ⁻⁶
	1.1	155	520	3.4	3.0	0.4	1.9	95	8.7 x 10 ⁻¹⁰
	1.1	150	1240	8.3	3.0	5.3	9.4	65	1.2 x 10 ⁻⁸
	3.0	150	520	3.5	3.0	0.5	2.0	90	1.0 x 10 ⁻⁸
	3.0	160	600	3.8	3.0	0.8	9.4	95	1.7 x 10 ⁻⁸
3	0.55	54	320	5.9	3.3	2.6	1.5	90	3.7 x 10 ⁻¹⁰
	0.55	66	820	12.4	3.3	9.1	9.0	43	1.3 x 10 ⁻⁹
	1.1	170	600	3.5	3.3	0.2	1.8	84	4.2 x 10 ⁻¹⁰
	1.1	180	1680	9.3	3.3	6.0	9.0	78	1.3 x 10 ⁻⁸
	3.0	150	800	5.3	3.3	2.0	2.0	90	3.9 x 10 ⁻⁸
	3.0	180	1320	7.3	3.3	4.0	9.5	76	7.7 x 10 ⁻⁸
4	0.55	70	39.9	0.57	0.03	0.54	0.19	73	3.1 x 10 ⁻¹¹
	0.55	50	347	6.94	0.03	6.91	2.5	35	9.8 x 10 ⁻¹⁰
	1.1	145	4.35	0.03	0.03	0.0	0.25	35	-----
	1.1	155	205	1.32	0.03	1.29	1.8	35	2.7 x 10 ⁻⁹
	3.0	165	4.95	0.03	0.03	0.0	0.18	32	-----
	3.0	145	55.1	0.38	0.03	0.36	1.9	32	2.7 x 10 ⁻⁹
5	0.55	35	21	0.6	0.0	0.6	0.47	89	8.6 x 10 ⁻¹¹
	0.55	48	24	0.5	0.0	0.5	0.69	58	7.1 x 10 ⁻¹¹
	0.55	76	175	2.3	0.0	2.3	1.7	61	3.3 x 10 ⁻¹⁰
	1.1	134	0.0	0.0	0.0	0.0	0.44	96	-----
	1.1	175	0.0	0.0	0.0	0.0	0.63	66	-----
	1.1	156	125	0.8	0.0	0.8	2.0	60	1.7 x 10 ⁻⁹
	1.1	170	238	1.4	0.0	1.4	2.0	58	2.9 x 10 ⁻⁹
	1.1	160	160	1.0	0.0	1.0	2.1	66	2.1 x 10 ⁻⁹
	1.1	142	170	1.2	0.0	1.2	2.3	66	2.5 x 10 ⁻⁹
	1.1	145	203	1.4	0.0	1.4	3.1	58	2.9 x 10 ⁻⁹
	3.0	128	88.9	0.7	0.0	0.7	0.86	91	1.3 x 10 ⁻⁸
	3.0	140	28.0	0.2	0.0	0.2	0.86	91	3.9 x 10 ⁻⁹
	3.0	122	12.2	0.1	0.0	0.1	3.3	62	1.9 x 10 ⁻⁹

48

*Unreliable

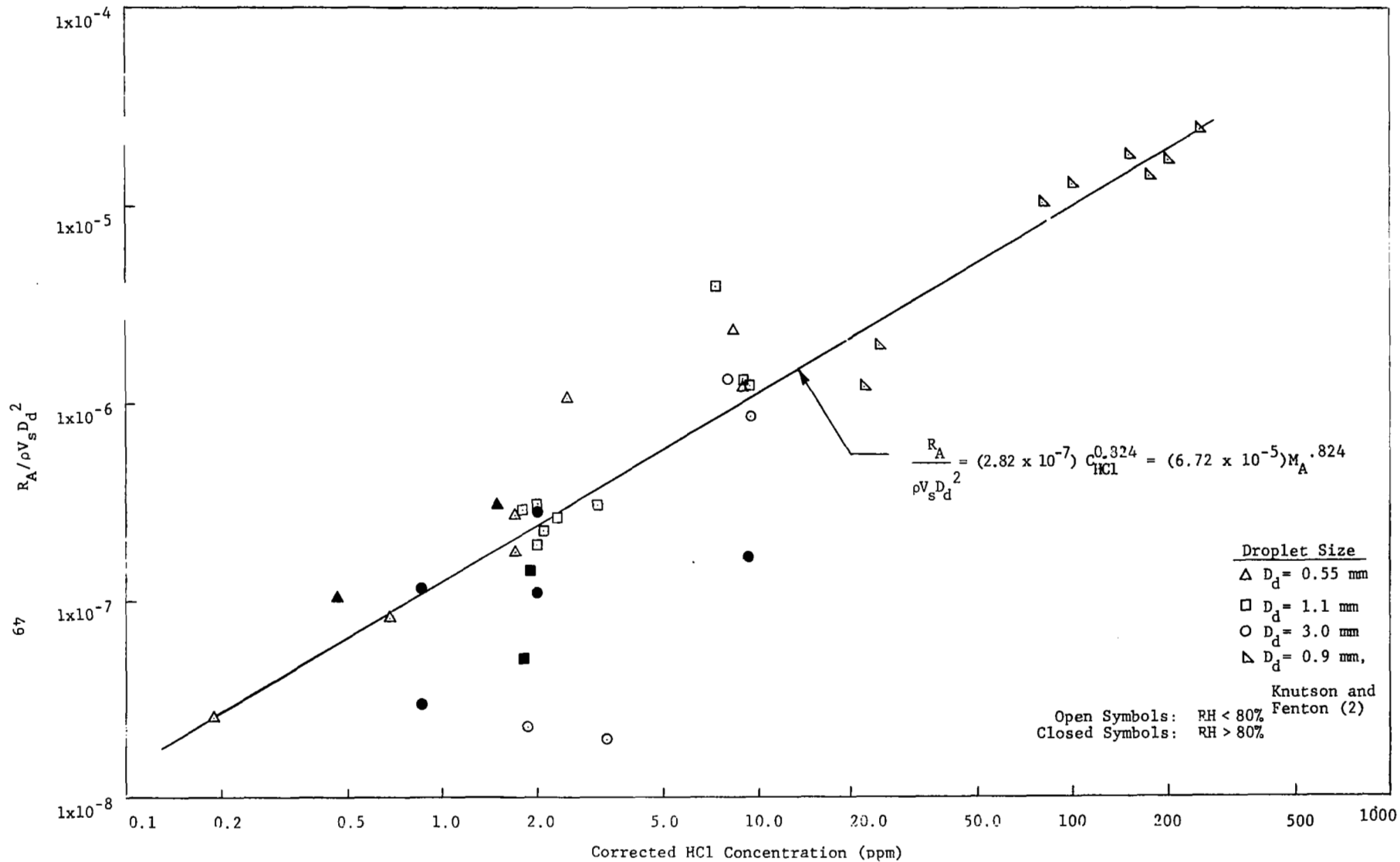


Figure 18

ROCKET EXHAUST HCl SCAVENGING DATA FOR MULTIPLE RAINDROP SIZES

The parameter is observed to generalize the scavenging data fairly well.

Error limits cannot be calculated for the scavenging data as simultaneous "blank" experiments were not conducted. However, one particular set of test conditions was repeated four times to determine precision within the experimental technique (rocket test number 5--1.1mm droplet diameter). The percent deviations are noted to be approximately 35% and may vary for the other two droplet sizes as the typical chlorine concentration levels vary. For the larger 3.0mm droplets, lower chlorine levels should mean reduced experimental precision while for the smaller 0.55mm droplets, experimental precision is probably enhanced.

Based on theoretical analysis, the relative humidity was thought to strongly influence the scavenging rate. The theory asserted that droplet growth was accelerated by the presence of HCl and, therefore, once cloud nucleation occurred, the HCl content should have been predominantly in the liquid phase for relative humidities greater than 80%. At this point, the scavenging rate was reduced because of the lower collision efficiency. In contrast to this assertion, the experimental data displayed no strong influence of R.H. on the HCl scavenging rate. High humidity did show a slight depression in scavenging rate, but the depression was within experimental errors. Further work relating to the influence of the rocket exhaust cloud constituents upon scavenging pure gaseous HCl is presented in the appendix.

Several scavenging experiments were conducted in the presence of fog. The experiments were conducted as follows. The experimental chamber was first filled with a visible fog generated with the commercial fog nozzle. Initially, the HCl detectors indicated that the HCl was predominantly gaseous. After approximately 10 seconds, the gaseous HCl concentration decreased until the dominant HCl phase was liquid HCl. This experiment was repeated several times during three rocket tests with the same results--virtually total transformation of the HCl to the liquid phase over a very short (5-15 seconds) time interval.

Droplets formed on the inner wall of the experimental chamber were checked for pH after approximately two minutes of exposure to the exhaust cloud (~ 2.0 ppm HCl). The pH determined by sensitized paper was about 3.1. The pH value was significantly greater than the unity value reported during field measurements by NASA-Langley. A plausible explanation is that the field measurements collected droplets grown in size promoted by the presence of HCl-mist formation. This explanation is also likely from consideration of the close proximity of the rain collection site to that of the launch vehicle.

4.1.2 Correlation of Scavenging Data

Due to information concerning the terminal settling velocity of raindrops as a function of diameter, an empirical correlation can be deduced from the experimental scavenging data. This section discusses the calculations leading to the final correlation.

Marshall and Palmer (19) presented an expression for raindrop concentration and size as follows:

$$C_{rd} = 0.08 \exp \left[\frac{-41D_d}{R^{0.21}} \right]$$

where

$$C_{rd} = \text{concentration of raindrops of diameter } D_d \text{ to } D_d + \Delta D_d, \left(\frac{\text{drops}}{\text{cm}^3} \right)$$

$$D_d = \text{raindrop diameter, (cm)}$$

$$R = \text{rainfall intensity, } \left(\frac{\text{mm}}{\text{m}} \right)$$

Dingle and Hardy (20) have evaluated the Marshall-Palmer expression for a number of raindrop size spectra and have determined the general validity of the expression on the average. Some individual rainfalls were noted to vary widely from the norm.

Gunn and Kinzer's (11) data were used for the terminal settling velocity of the raindrops. Figure 19 shows the discrete points comprising the data and a power curve selected to

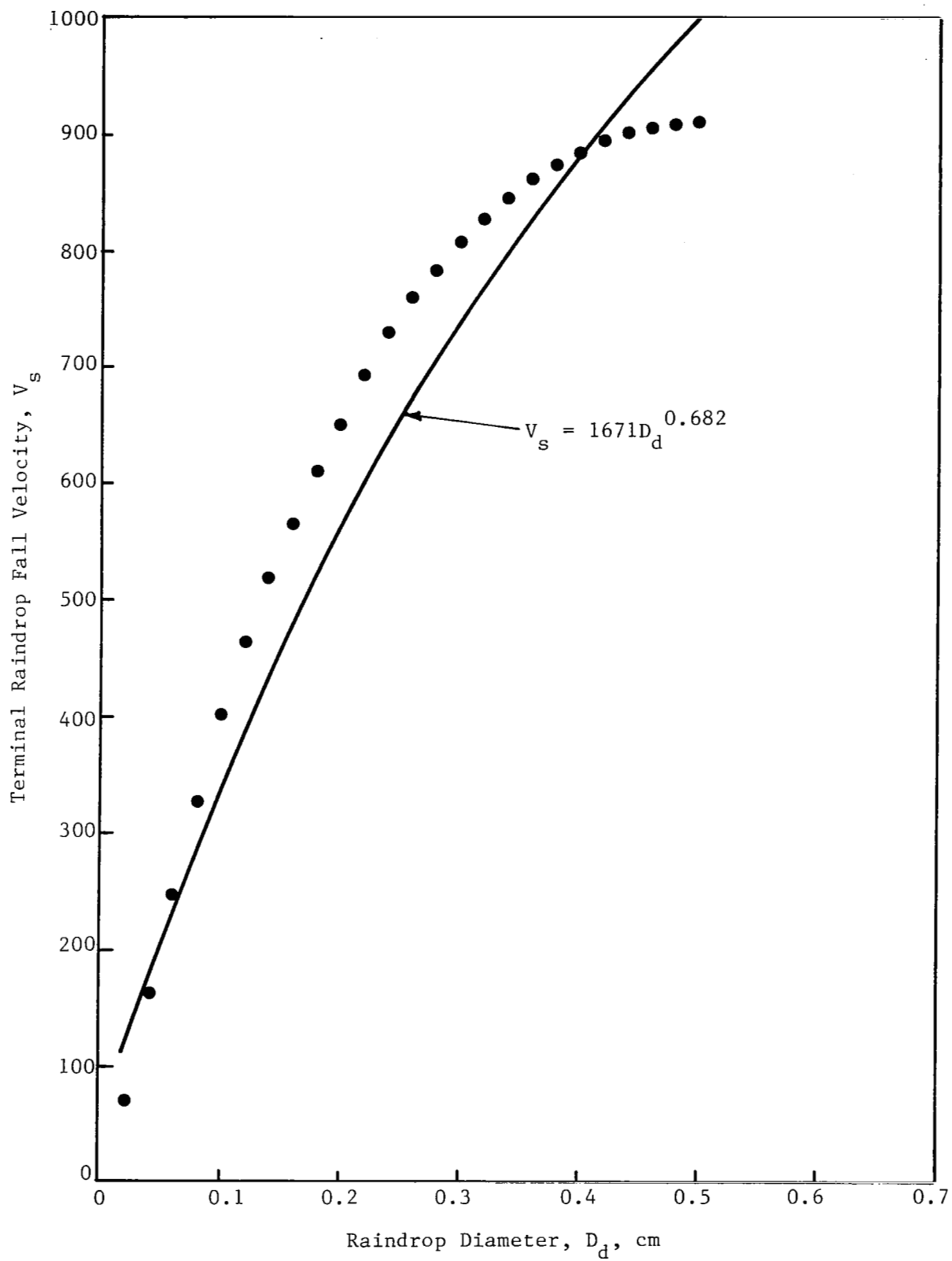


Figure 19

RAINDROP TERMINAL FALL VELOCITY AS DETERMINED
BY GUNN AND KINZER (11)

fit the data where the coefficient of determination was 0.93--a relatively good fit. The terminal velocity data was not connected for temperature, relative humidity, or local wind velocity.

The HCl scavenging data presented in Figure 18 is fitted by a power curve as follows:

$$\frac{R_A}{\rho V_s D_d^2} = (6.72 \times 10^{-5}) M_A^{0.824}$$

where M_A is the mass concentration of HCl (g/m^3). Defining Q as the rate of removal of HCl from a cubic meter of exhaust cloud, it then follows that

$$Q = \int_{D_d} R_A(D_d) C_{rd}(D_d) dD_d.$$

Now, defining the washout coefficient, Λ , as the HCl removal rate over the HCl concentration, Λ then becomes

$$\Lambda = \frac{1}{M_A} \int_{D_d} R_A(D_d) C_{rd}(D_d) dD_d.$$

Substituting the experimental correlation and the power function for the raindrop terminal velocity, the following integral results

$$\Lambda = (8.98 \times 10^{-3}) \rho M_A^{0.176} \int_{D_d} D_d^{2.682} \exp \left[\frac{-41D_d}{0.21R} \right] dD_d.$$

Carrying-out the integration utilizing numerical procedures (increment size for $D_d = 0.04$ cm) for several rainfall intensities varying from 1.0 to 30.0 mm/hr. yields

$$\Lambda = (4.21 \times 10^{-8}) \rho M_A^{0.176} R^{0.773}$$

and under standard atmospheric conditions for ρ gives

$$\Lambda = (5.12 \times 10^{-5}) M_A^{0.176} R^{0.773}.$$

The above empirical relationship is different from the earlier reported relations (1, 2)

$$\Lambda = (8.3 \times 10^{-5}) R^{0.567}, \text{ Knutson and Fenton (2)}$$

$$\Lambda = (1.11 \times 10^{-4}) R^{0.625}, \text{ Pellet (1)}$$

by virtue of the non-linearity. However, the approach taken here to deduce the HCl washout correlation is based strictly on the data obtained. Both previous investigations assumed the form of the Frossling correlation and fitted the data accordingly, hence the perfect linear correlation. The fact that the exponent of M_A is relatively small--0.176--the influence of M_A on Λ is weak over the HCl concentration range tested. The total influence of the HCl concentration on the washout coefficient is only about a factor of 2.1 and is seen to be within the errors incorporated within the experimental data. In this sense, the relation found here supports the earlier correlations.

4.2 Absorption Tests

The absorption of rocket exhaust HCl was measured for several liquid surfaces typical of the region near Cape Kennedy. The liquids tested included sea water, brackish water, distilled water, and a 0.05 normal solution of NaOH as a reference. The composition of these liquids and the procedures used during the experiments was described earlier within this report.

Table 7 lists the collected data and the calculated results for the deposition velocity. Immediately apparent from the data is the extremely large deposition velocities and HCl mass fluxes into the sea and brackish water surfaces. These values are unreliable because of the high chlorine-ion background values (inherently present for these liquids) coupled with chlorine-ion analysis techniques of insufficient sensitivity. As a consequence, experiments with both sea and brackish water were dropped from the test sequence.

Reviewing the data from only the distilled water and the 0.05 normal solution of NaOH, the deposition velocities (and HCl mass flux values) are reasonable, relative to comparable gaseous

Table 7

ROCKET EXHAUST HCl ABSORPTION TEST RESULTS

Rocket Number	Exposed Material	Vol. (ml)	Time Interval (min)	HCl* Conc.		Reference Cl ⁻ Conc. (µg/ml)	Uncorrected Cl ⁻ Conc. (µg/ml)	Corrected Cl ⁻ Conc. (µg/ml)	HCl Flux F (g/m ² sec)	Deposition Velocity, Vg (cm/sec)	Normalized Vg
				(ppm)	(mg/m ³)						
2	Distilled H ₂ O	200	10	24	36	2.1	5.5	3.4	8.79 x 10 ⁻⁵	0.24	0.22
	Brackish H ₂ O	236	10	30	45	13,900	13,200	-700	-----	--	--
	Sea H ₂ O	250	10	27	41	25,900	40,000	14,100	2.56 x 10 ⁻¹	1100	1000
	Reference NaOH (0.05 Normal)	248	10	26	39	18.9	32.9	14.0	4.48 x 10 ⁻⁴	1.1	1.0
3	Distilled H ₂ O	230	10	26	39	2.4	7.2	4.8	1.14 x 10 ⁻⁴	0.33	0.31
	Brackish H ₂ O	280	10	31	48	11,100	13,900	2,800	7.78 x 10 ⁻²	180	170
	Sea H ₂ O	260	10	29	45	30,200	40,400	10,200	2.63 x 10 ⁻¹	660	610
	Reference NaOH (0.05 Normal)	190	10	29	45	20.6	42.7	22.1	4.17 x 10 ⁻⁴	1.1	1.0
4	Distilled H ₂ O	200	30	7.9	11.9	0.015	2.52	2.50	1.90 x 10 ⁻⁵	0.21	0.78
	Reference NaOH (0.05 Normal)	235	30	7.1	10.7	1.60	4.17	2.57	2.27 x 10 ⁻⁵	0.27	1.0
5	Distilled H ₂ O	232	20	10.2	15.8	0.0	4.1	4.1	4.08 x 10 ⁻⁵	0.35	0.84
	Reference NaOH (0.05 Normal)	275	20	8.8	13.0	0.5	4.0	3.5	4.14 x 10 ⁻⁵	0A1	1.00

*Time averaged values over time interval for absorption experiment.

pollutants. Moreover, the normalized (reference solution) deposition velocity ratio is reduced for the high HCl concentrations. The reduction in the deposition velocity ratio corresponds in magnitude to the change in normalized HCl concentration.

Also note, as shown in Figure 20, that the HCl deposition velocity for NaOH is concentration dependent, while the deposition velocity for H₂O is not dependent on the concentration. An explanation for this may be that since the absorption surface is stagnant, the liquid immediately below the free surface becomes saturated at the higher HCl concentrations more readily, thus restricting continued absorption of HCl. With the lower HCl concentration above the free surface, longer exposure times are required for saturation to occur therefore absorbing a relatively larger amount of HCl compared to the reference surface over the same time interval.

4.3 Plant Uptake Tests and Growth Response

The exposure of standard test plants, a monocotyledonous - corn, Zea mays, and a dicotyledonous - soybean, Glycine max, were used to determine the amount of HCl uptake during a specified period of exposure. A preliminary test was conducted at the conclusion of the experimental test sequence to determine real-time growth response.

Related work has been recently reported or is under way in relation to plant injury caused by exposure to the rocket exhaust. The Kennedy Space Center has sponsored investigations on plant injury both at the Florida Technological Institute and North Carolina State University. The Florida work used scale-model rockets to generate an exhaust cloud within a Teflon tent enclosing the vegetation of interest near the launch site. Brown spotting on the plants was observed but the HCl-concentration measurement was considered unreliable (21).

The work at North Carolina State University is being currently managed by Dr. Walter Heck (22). Experimental results are not available from this study. The experiments are planned to evaluate injury to a number of plant species within specially designed

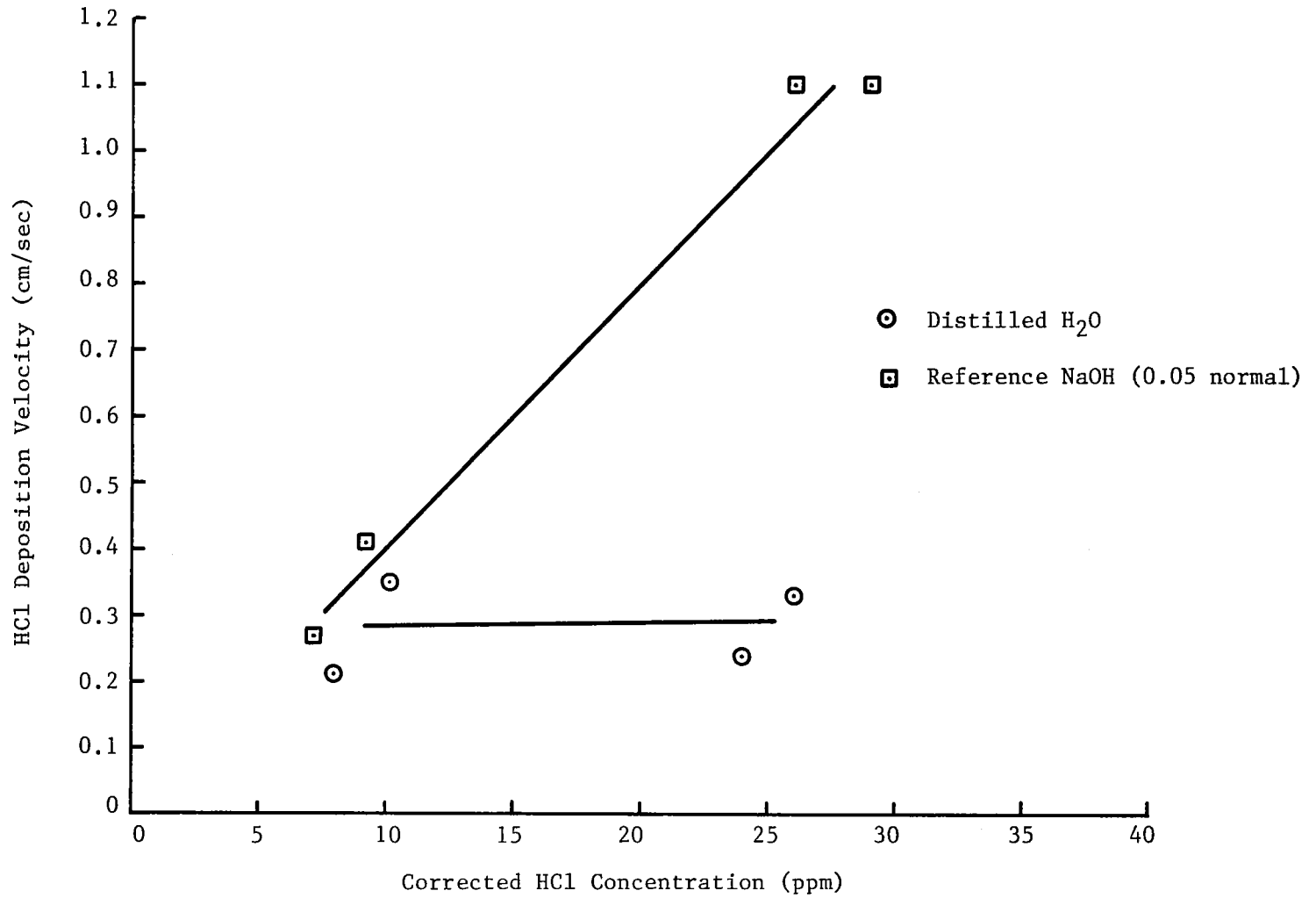


Figure 20

ROCKET EXHAUST HCl DEPOSITION VELOCITY VARIATION WITH HCl CONCENTRATION

exposure chambers. Lerman et. al. (23), while at the University of California at Riverside, exposed numerous plant species to pure gaseous HCl and found Geraniums to be most sensitive to HCl exposures.

The experiments at IITRI, therefore, were not directed toward the determination of plant injury, but rather, toward the uptake of HCl. This concern stems from the requirement for reliable HCl "sink" terms comprising the multi-layer diffusion model describing the dynamics of the ground exhaust cloud.

Table 8 shows the measurements made with the test plants. The levels of Cl^- concentration on a dry weight basis from the rocket tests measured with a specific-ion electrode are suspiciously high. The last test (number 4) utilized a colorometric method for Cl^- analysis and is considered more reliable, but appears also high. The uncertainty in the colorometric measurements was approximately 15%. Applying the 15% uncertainty to the last test, observe that the magnitude of the errors overlap, thus rendering the net Cl^- uptake data unreliable. Note, however, that for all the test data, the trend of increased Cl^- concentration is not violated. Therefore, the tests can be used to establish overall trends.

In examining the data from corn, a direct correlation was found between plant age and Cl^- uptake: the younger the plant, the higher was the Cl^- concentration on a dry weight basis. This is consistent for each of the first three tests. With soybeans, no correlation with age was observed. The net average HCl uptake for corn was approximately 6000 $\mu\text{g/g}$ dry weight for soybeans, approximately 1000 $\mu\text{g/g}$. HCl uptake in soybeans was reduced by a factor of approximately six as compared to the monocotyledonous plant represented by corn. These results are considered tentative because of the limited number of tests performed.

The determination of real-time growth response to rocket exhaust exposure is a first step in examining the more complex plant responses which include among others reproduction and yield.

Table 8

SUMMARY OF TEST PLANTS HCl UPTAKE MEASUREMENTS

Rocket Number	Plant Type	Age* (days)	Exposure Time (min)	Rel. Hum. (%)	Experimental Chamber HCl Concentration (ppm)	Dry Weight (g)	Total Cl ⁻ (μg)	Total Cl ⁻ /Dry Wt. (μg/g)	Net Cl ⁻ /Dry Wt. (μg/g)	Comments
1	beans	14	20	50	8	3.404	51,320	15,100	1,600	
	beans	14	control			2.113	28,560	13,500		
	corn	14	20	50	8	2.690	101,160	37,600	17,000	
	corn	14	control			4.273	87,960	20,600		
2	beans	24	20	90	10	2.069	20,880	10,000	2,000	leaves pointed downward approximately 45°
	beans	24	control			2.877	23,040	8,000		
	corn	24	20	90	10	3.952	108,100	27,350	1,750	
	corn	24	control			3.254	83,440	25,600		
3	beans	14	20	80	10	0.9019	6,850	7,600	910	leaves pointed downward approximately 45°
	beans	14	control			0.8346	5,580	6,690		
	corn	14	20	80	10	1.2984	19,200	14,800	4,700	wrinkles on leaf edges
	corn	14	control			0.8656	8,770	10,100		
4	beans	21	20	75	2	2.5	14,300	5,700	800	leaves pointed downward during exposure
	beans	21	control			3.2	15,700	4,900		
	corn	21	20		2	4.4	105,200	23,900	1,800	brown spots increased in area of leaf tips
	corn	21	control			3.4	75,100	22,100		

*Measured from time of planting.

To gain some insight in this area, a preliminary growth response experiment was conducted with soybeans in which internode elongation was measured. Two sets of plants, the controls and plants to be exposed were placed in corresponding chambers, the experimental chamber and a temporary chamber, where identical light and temperature conditions were maintained. Sensitive displacement transducers were placed into the chambers and internode elongation of two single plants was continuously recorded, before, during and after the exposure to the rocket exhaust.

Figure 21 shows the results of the growth response measurement. Immediately before and during the exposure to the rocket exhaust, the elongation rate decreased to approximately 0.6 of the overall elongation rate of the experimental plant. At the midpoint of the 20 minute exposure, the elongation rate dropped to 1/3 of this rate and approached slowly a zero rate. While it is tempting to ascribe this decrease in the elongation rate to the rocket exhaust, further tests are required.

The elongation rate of the control was approximately two times higher than that of the experimental plant throughout the test period. While such variations in elongation rates are not uncommon, it excludes further interpretation of the results without additional test. The manifestation of the growth response in other plants after HCl exposures also remains to be investigated.

4.4 Metallic Corrosion Tests

Differential weight determinations were used to ascertain the advent of significant corrosion. Table 9 lists all the data obtained throughout the entire test program including visual observations. All the coupons received a single exposure to the rocket exhaust effluent. To readily compare the data, Figure 22 was prepared.

In discerning trends from the differential weight data, note first the general lack of positive increase. Usually when significant corrosion occurs, weight gains are measured. Since this

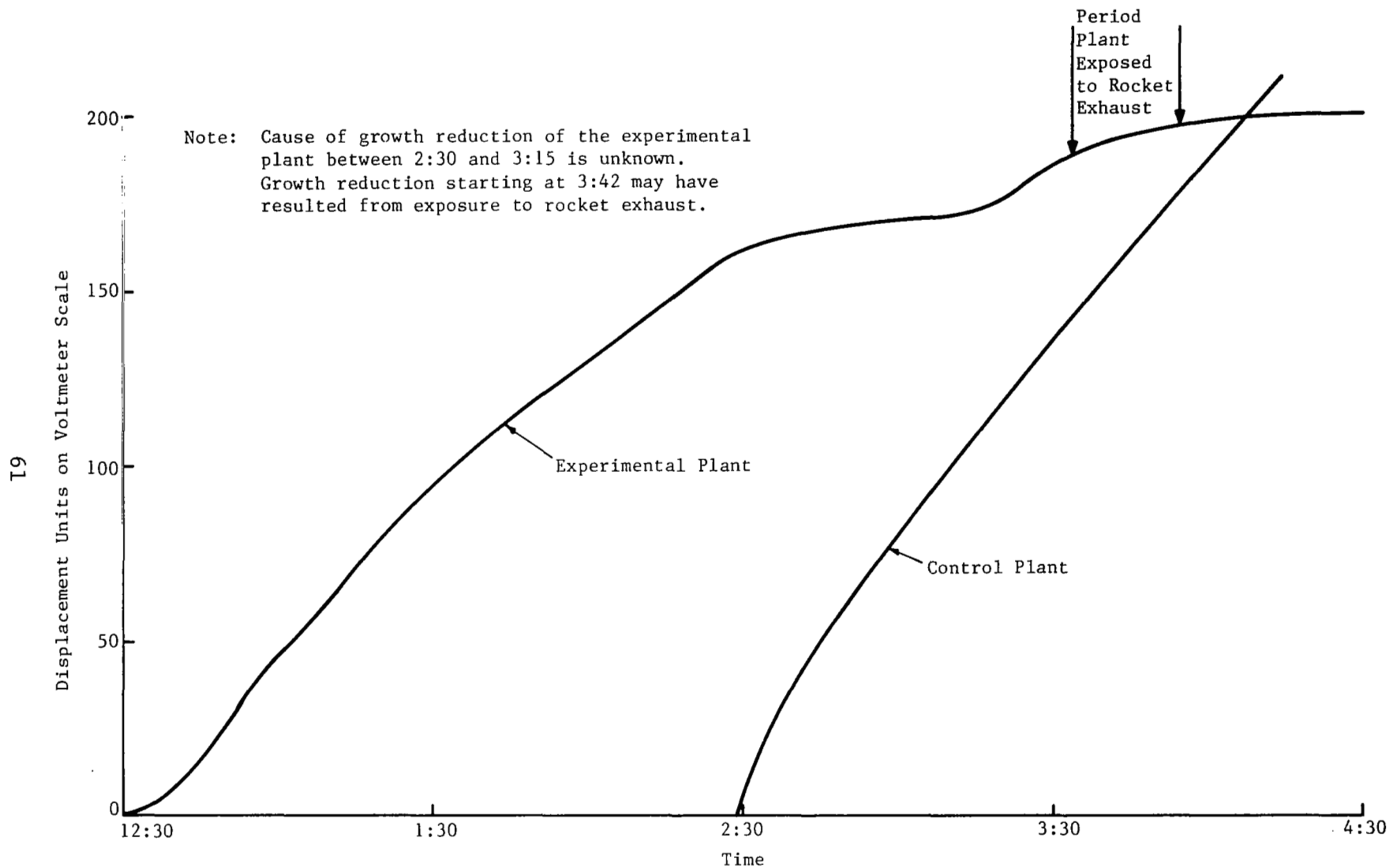


Figure 21

GROWTH RESPONSE OF SOYBEAN SEEDLINGS TWO WEEKS AFTER GERMINATION

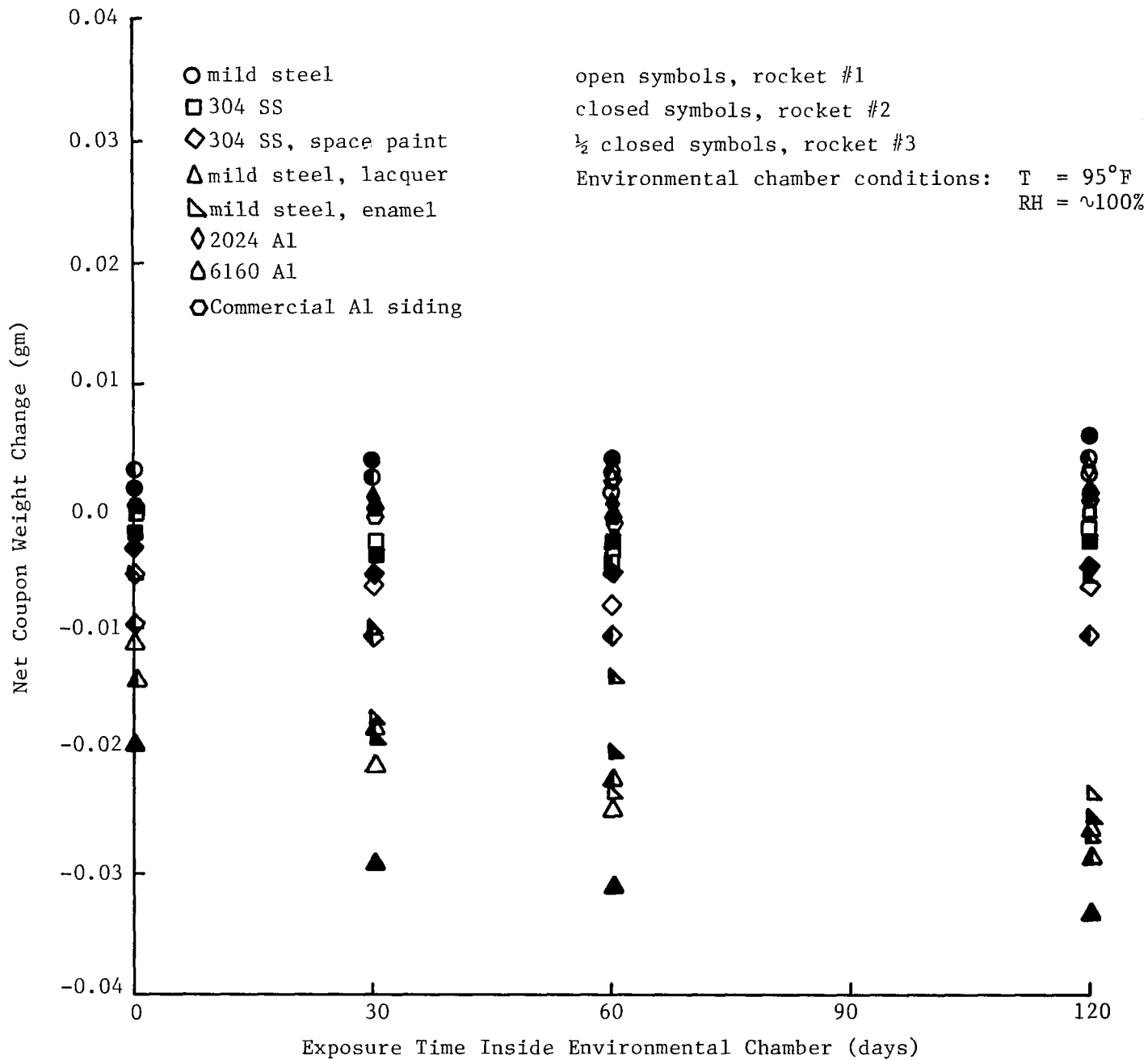


Figure 22

NET COUPON WEIGHT CHANGES VERSUS LENGTH OF EXPOSURE TIME

Table 9

MEASURED WEIGHT CHANGES ASSOCIATED WITH EXPOSED METAL COUPONS

Rocket Number	Sample Type*	Initial Coupon Weight (gm)	Coupon Wt. Change After Exposure (gm)	Coupon Wt. Change After 30 Days (gm)	Coupon Wt. Change After 60 Days (gm)	Coupon Wt. Change After 120 Days (gm)	Exposure Conditions		Comments
							%RH	HCl Conc. (ppm)	
1	mild steel	54.6085	+0.0012	0.0000	+0.0010	+0.0025	~50	8	rusted in environmental chamber
	304 SS	70.1722	-0.0007	-0.0031	-0.0036	-0.0019	~50	8	
	304 SS, space paint	72.9200	-0.0053	-0.0066	-0.0081	-0.0068	~50	8	coating thickness = 8 mils
	mild steel lacquer	55.5674	-0.0112	-0.0211	-0.0249	-0.0260	~50	8	
	mild steel enamel	57.4726	-0.0056	-0.0171	-0.0234	-0.0236	~50	8	
	2024 aluminum	22.0987	+0.0020	+0.0027	+0.0013	+0.0029	~50	8	
	6160 aluminum	21.2319	-0.0002	-0.0006	-0.0017	+0.0006	~50	8	
	commercial Al siding	3.4024	-0.0004	-0.0001	-0.0016	+0.0001	~50	8	
2	mild steel	53.8593	+0.0014	+0.0037	+0.0038	+0.0056	~90	10	heavy rust in environmental chamber
	304 SS	69.8119	-0.0021	-0.0040	-0.0029	-0.0029	~90	10	
	304 SS, space paint	72.9200	-0.0036	-0.0056	-0.0057	-0.0052	~90	10	coating thickness = 8 mils
	mild steel, lacquer	54.0404	-0.0195	-0.0294	-0.0311	-0.0333	~90	10	paint chipped during test
	mild steel, enamel	56.8873	-0.0052	-0.0189	-0.0201	-0.0255	~90	10	
	2024 aluminum	22.2523	+0.0003	+0.0007	-0.0004	-0.0014	~90	10	
	6160 aluminum	20.2721	-0.0004	-0.0004	-0.0013	+0.0006	~90	10	
	commercial Al siding	3.4697	-0.0006	-0.0007	-0.0015	+0.0012	~90	10	
3	mild steel	53.2960	+0.0029	+0.0024	+0.0029	+0.0038	~80	10	rusted in environmental chamber
	304 SS	69.1093	-0.0014	-0.0033	-0.0034	-0.0038	~80	10	
	304 SS, space paint	71.7960	-0.0099	-0.0108	-0.0107	-0.0107	~80	10	coating thickness = 8 mils
	mild steel, lacquer	54.4606	-0.0140	-0.0176	-0.0222	-0.0286	~80	10	
	mild steel, enamel	56.3894	-0.0039	-0.0097	-0.0138	-0.0269	~80	10	
	2024 aluminum	22.1002	+0.0029	+0.0024	+0.0021	+0.0027	~80	10	
	6160 aluminum	20.5965	+0.0003	-0.0001	-0.0008	-0.0002	~80	10	
	commercial Al siding	3.5465	-0.0004	-0.0004	-0.0001	-0.0002	~80	10	
4	mild steel	56.0566	+0.0003	-0.0010	+0.0004	---	~75	2	slight rusting after 30 days
	304 SS	68.8626	-0.0019	-0.0034	-0.0024	---	~75	2	
	304 SS, space paint	73.6475	-0.0055	-0.0076	-0.0075	---	~75	2	coating thickness = 8 mils
	mild steel, lacquer	54.9344	-0.0184	-0.0257	-0.0266	---	~75	2	
	mild steel, enamel	57.8603	-0.0249	-0.0249	-0.0321	---	~75	2	
	2024 aluminum	21.3193	-0.0010	-0.0012	-0.0005	---	~75	2	
	6160 aluminum	20.1279	-0.0005	-0.0007	-0.0006	---	~75	2	
	commercial Al siding	3.5052	-0.0001	-0.0003	0.0000	---	~75	2	

*Table 5 gives details regarding coupon metallurgical data preparation

did not occur with the exposed metallic coupons, significant corrosion did not occur during the 120 day incubation period. Importantly, the aluminum siding remained very constant, showing no signs of corrosion. In contrast, several coupons lost a discernable weight--both the painted mild steel coupons--but showed no rust as did the unpainted mild steel. However, all the weight differentials are small and even the trends cited must be considered tentative.

4.5 Characterization and Scavenging of Rocket Exhaust Aluminum Oxide Dust

Three instruments were used to obtain the particle size data: the electrical aerosol analyzer (Thermo-Systems Model 3030), a light-scattering instrument (Royco 220 and 245), and a cascade impactor (Andersen). Each instrument is operable over the different particle diameter size ranges as indicated:

- electrical aerosol analyzer, 0.01 to 0.7 μm
- light scattering, 0.5 to 5.0 μm
- cascade impactor, 1.0 to 9.0 μm

Particle size differentiation with the EAA and the light-scattering instruments was based on the geometric size of the particle while size differentiation with the cascade' impactors was based on particle inertia.

During the first scavenging test (Rocket #1) a light-scattering instrument was employed (Royco 220). Use of this particular instrument was restricted by its low particle loading capability--the maximum particles concentration that can be accommodated is 5 particles/cm³. However, the particle size pertaining to the maximum number concentration can be approximated and is given below.

<u>Time After Rocket Ignition (min)</u>	<u>Approx. Particle Size at Max Concentration (μm)</u>	<u>Concentration of HCl (ppm)</u>
15	2.5	8.0
90	2.0	3.0
120	1.7	1.2

Data for the second scavenging test were taken during the third rocket firing. Figure 23 shows the data (corrected for background) as obtained by the EAA and the light-scattering instrument (Royco Model 245). This light-scattering instrument had adequate particle loading capability for the rocket exhaust cloud being tested.

As can be seen in Figure 23, a substantial number of particles occur within the submicron particle size range. Note that an inflection point occurs at approximately $0.7 \mu\text{m}$, thus suggesting a bimodal particle size distribution. This is reasonable as the complicated combustion process within the rocket nozzle generates particles by both gaseous condensation of alumina and by the dispersion of molten alumina. In addition, Dr. Varsi's data have been obtained through Ron Dawbarn at ARO, Inc. where a Titan III exhaust cloud was sampled with a specially instrumented aircraft (including an EAA) approximately 10 minutes after launch. Varsi shows an inflection point at $0.5 \mu\text{m}$ --very comparable to our own $0.7 \mu\text{m}$ inflection point. The total particle number concentration of the sampled Titan III exhaust cloud was 3×10^4 particles/cm³ whereas within our experimental chamber at 100 minutes after ignition the concentration was 1.4×10^5 particles/cm³ and at 280 minutes, 1.2×10^5 particles/cm³. The number concentrations differ by a factor of four. Not known is the HCl concentration within the exhaust cloud of the Titan III; this information can be used to check the "dilution factor" of four. Based on the characterization of the Al_2O_3 particles, the exhaust from the JPL scale rocket is considered as an accurate replica of the cloud generated by a full-sized rocket. The reduction in particle count with time is best accounted for by coagulation of the submicron particles as observed in Figure 23.

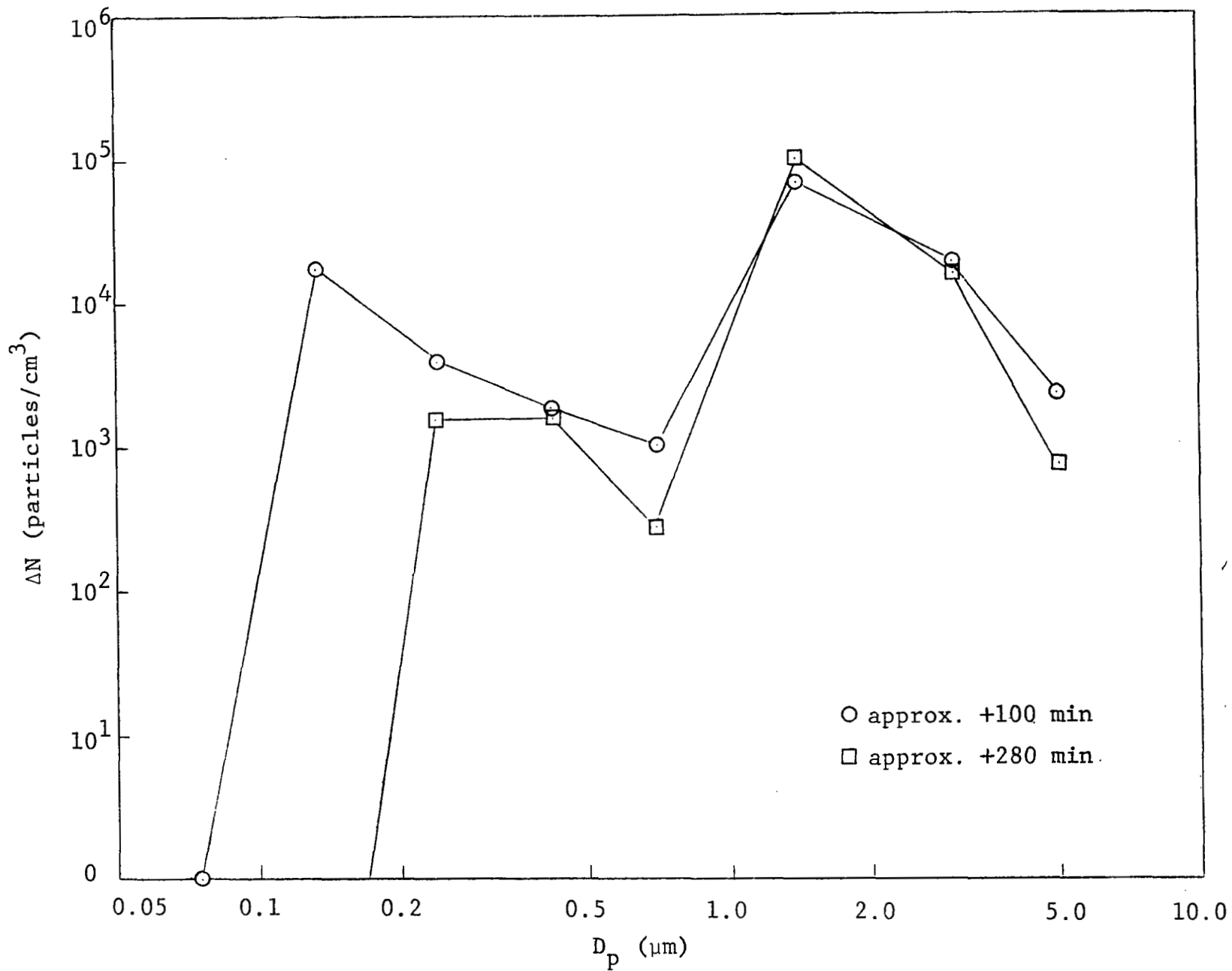


Figure 23 Al_2O_3 PARTICLE SIZE DATA FOR SECOND SCAVENGING TEST

Data from the Andersen impactor (flow rate = 28.2 lpm) are given below.

<u>Stage Number</u>	<u>Particle Size Range Collected (μm)</u>	<u>Mass Collected (mg)</u>
1	>9	0.8
2	5.5 - 9	0.2
3	3.3 - 5.5	0.1
4	2 - 3.3	0.2
5	1 - 2	1.0
6	<1	0.5

Note that, based on particle number the mean size is again in the range of 1 to 2 μm . This collaborates the data obtained by the other two techniques.

Measurements of particle size were also performed on the third rocket firing. The Royco Model 245 and the Andersen impactor were used. The data from the Royco are shown in Figure 24 and the Andersen data given below.

<u>Stage Number</u>	<u>Particle Size Range Collected (μm)</u>	<u>Mass Collected (mg)</u>
1	>9	0.0
2	5.5 - 9	0.0
3	3.3 - 5.5	0.1
4	2 - 3.3	0.1
5	1 - 2	0.3
6	<1	0.0

The particle size data obtained support the data obtained during earlier scavenging tests.

During the last scavenging experiments, a sample of collected rain drops, 1.1 mm in diameter, was set aside for analysis of the entrained Al_2O_3 particles. Figure 25 displays the two particle number distributions--both airborne Al_2O_3 particles at the time of the experiment and the Al_2O_3 particles in the rainwater. The plot indicates that the droplets scavenge a larger proportion of the smaller submicron particles than the larger particles.

The number concentration of Al_2O_3 particles during the scavenging experiment was 5.4×10^4 particles/cm³ as measured by the light-scattering technique. The particle concentration within the collected rain was 3.5×10^5 particles/cm³--approximately an

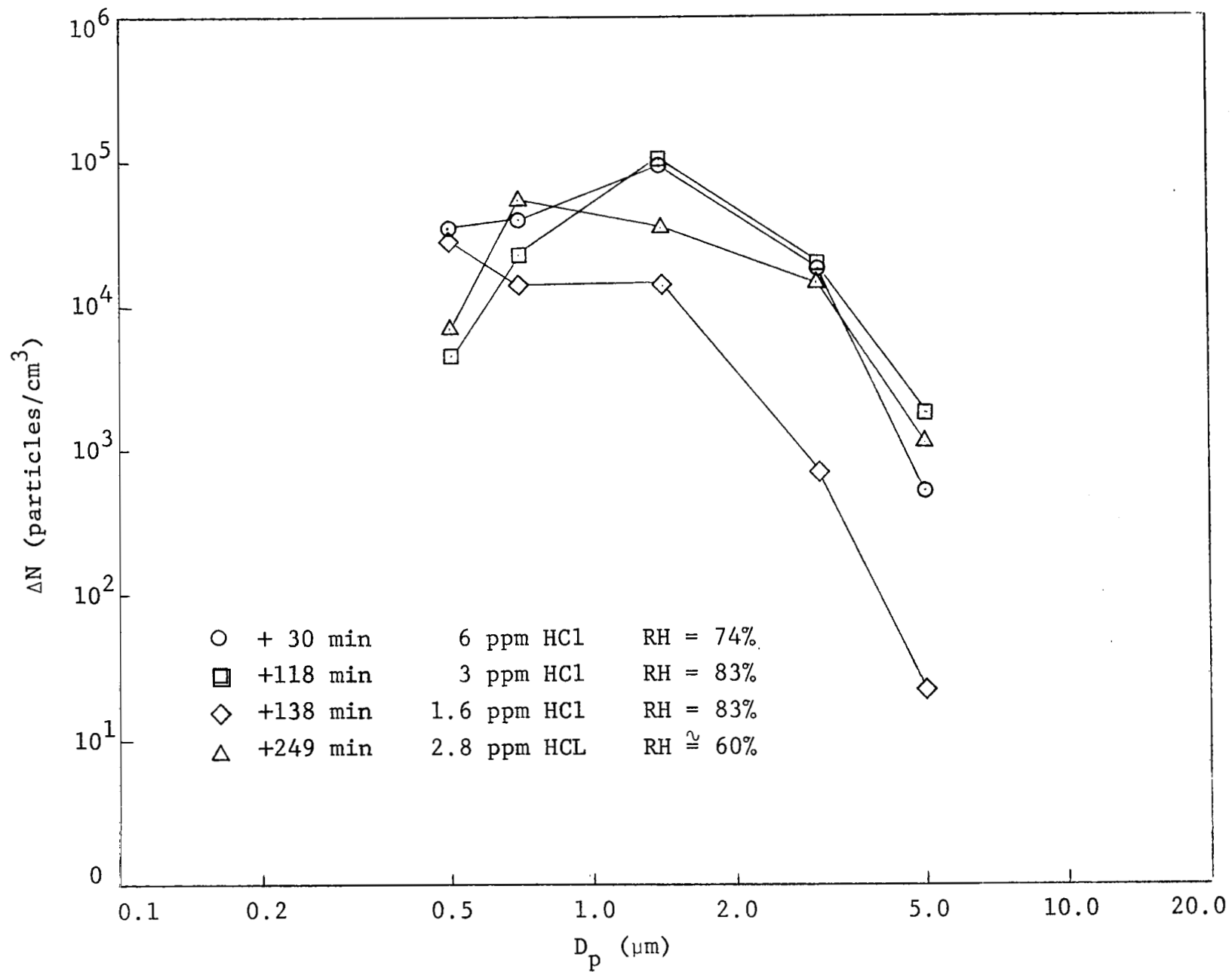


Figure 24 Al_2O_3 PARTICLE SIZE DATA FOR THIRD SCAVENGING TEST

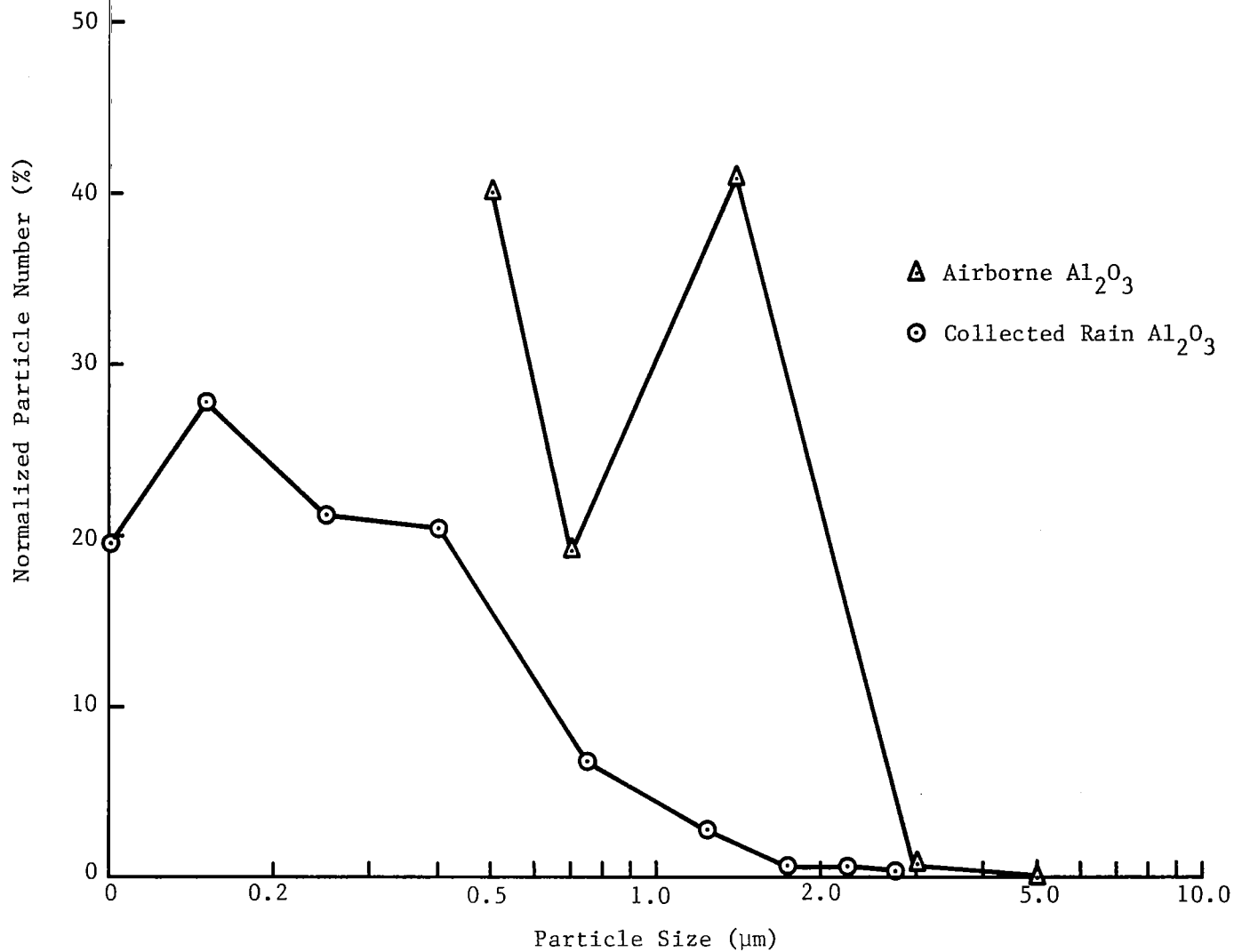


Figure 25

Al₂O₃ PARTICLE SIZE DISTRIBUTIONS BASED ON NUMBER FOR BOTH AIRBORNE AND COLLECTED RAIN (1.1 mm DIAMETER)

order-of-magnitude greater than the airborne concentration. This result appears questionable as the volume any one drop sweeps through during the fall is only 1.24 cm^3 . For the droplet to collect the measured number of particles, the effective volume swept must be about ten times as great. A tentative explanation is the Al_2O_3 aerosol is electrically charged--as are most combustion aerosols--in such a way as to be attracted to the falling droplets. [Another plausible explanation may be added collection due to the eddy currents created by the falling droplets.] This experiment was conducted only once to demonstrate Al_2O_3 scavenging. Further investigation of Al_2O_3 scavenging would require significant improvement of the experimental procedure used here while maintaining the use of actual rocket exhaust to conduct the experiment.

Figures 26 and 27 are photomicrographs from a scanning electron microscope showing the Al_2O_3 particles collected by the raindrops. The non-spherical particles are not Al_2O_3 particles, but filter debris resulting from sample preparation. The crystalline material adjacent to a number of the Al_2O_3 particles contains significant quantities of chlorine (as determined by SEM microprobe) and appears to be a chlorine-containing salt. Other particles not possessing adjacent crystals may not be properly oriented, or, indeed, may not have adjoining chlorine crystals. An explanation for the adjacent crystals is not apparent.

5. CONCLUSION

Rocket exhaust HCl scavenging tests, surface corrosion, and uptake studies were undertaken experimentally. The conclusions presented here are developed and discussed within the text of this report. The conclusions are as follows:

1. The washout coefficient for HCl scavenging determined empirically is:

$$\Lambda = (5.12 \times 10^{-5}) M_A^{0.176} R^{0.773}$$

The nonlinearity effect of the $M_A^{0.176}$ factor is weak, varying only a factor of two over the range of HCl concentrations tested--0.2 to 10.0 ppm. This factor of two is overshadowed by the uncertainty comprising the experimental data.

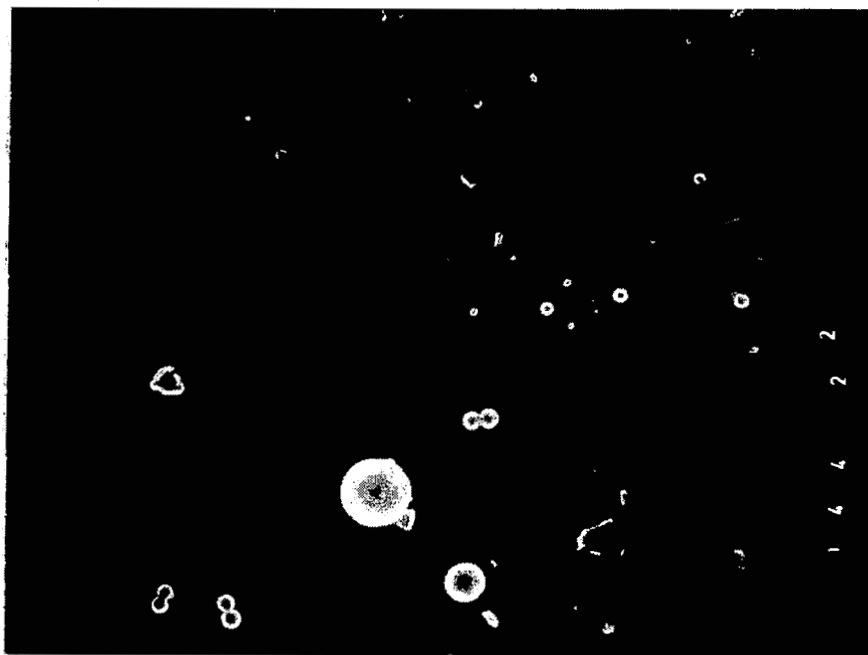


Figure 26

PHOTOMICROGRAPHS SHOWING Al_2O_3 PARTICLES COLLECTED BY
1.1 mm RAINDROPS AT 3,000X MAGNIFICATION

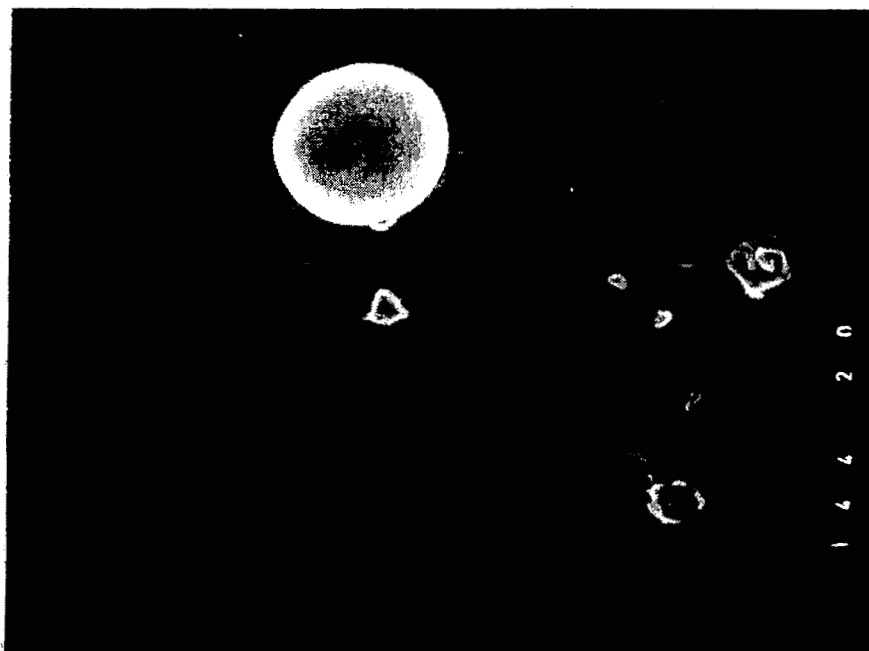


Figure 27

PHOTOMICROGRAPHS SHOWING Al_2O_3 PARTICLES COLLECTED BY
1.1 mm RAINDROPS AT 10,000 MAGNIFICATION

2. The surface uptake (calculated deposition velocities) rates for distilled water is less than the reference 0.05 normal NaOH solution and concentration dependent. Measurement of sea water and brackish water HCl deposition velocity is untenable due to inherently high chlorine background values.
3. Plant HCl uptake measurements utilizing corn and soybeans indicate significant uptake trends. Plant age effectively correlates the corn data: younger the plant age, the higher the Cl^- concentration on a dry weight basis. (There was no apparent correlation of plant age and HCl uptake for the soybeans.) Real-time growth response of soybeans occurs with HCl exposure of 20 minutes duration.
4. No significant corrosion is apparent from the metallic coupon corrosion experiments.
5. Particle size characteristics of Al_2O_3 small-scale rocket (227 g) is comparable to particle size data from full size rockets. It was tentatively found that raindrops effectively scavenge Al_2O_3 particulate material.

Appendix A

PURE GASEOUS HCl SCAVENGING

PURE GAS HCl SCAVENGING

At the conclusion of the last rocket exhaust scavenging test, pure HCl was introduced to the experimental chamber via lecture bottles pressurized with HCl. Three rain drop sizes were tested-- 0.55 mm, 1.1 mm, and 3.0 mm--with the results shown in Figure A-1. Immediately apparent is the lack of agreement with the empirical correlation resultant from the rocket exhaust scavenging data (an order-of-magnitude below the pure gaseous HCl scavenging data). Experiments with actual rocket exhaust constituents are, therefore, seen as highly significant.

The experimental conditions consisted of high relative humidities, in excess of 95%. And, indeed, here an extremely visible and persistent acid-mist was formed with the introduction of pure HCl into the experimental chamber. This acid-mist was not visible or detected with the instrumentation under rocket exhaust HCl. Apparently, the interacting constituents of the rocket exhaust cloud serve to suppress the scavenging rate of HCl for a given HCl concentration.

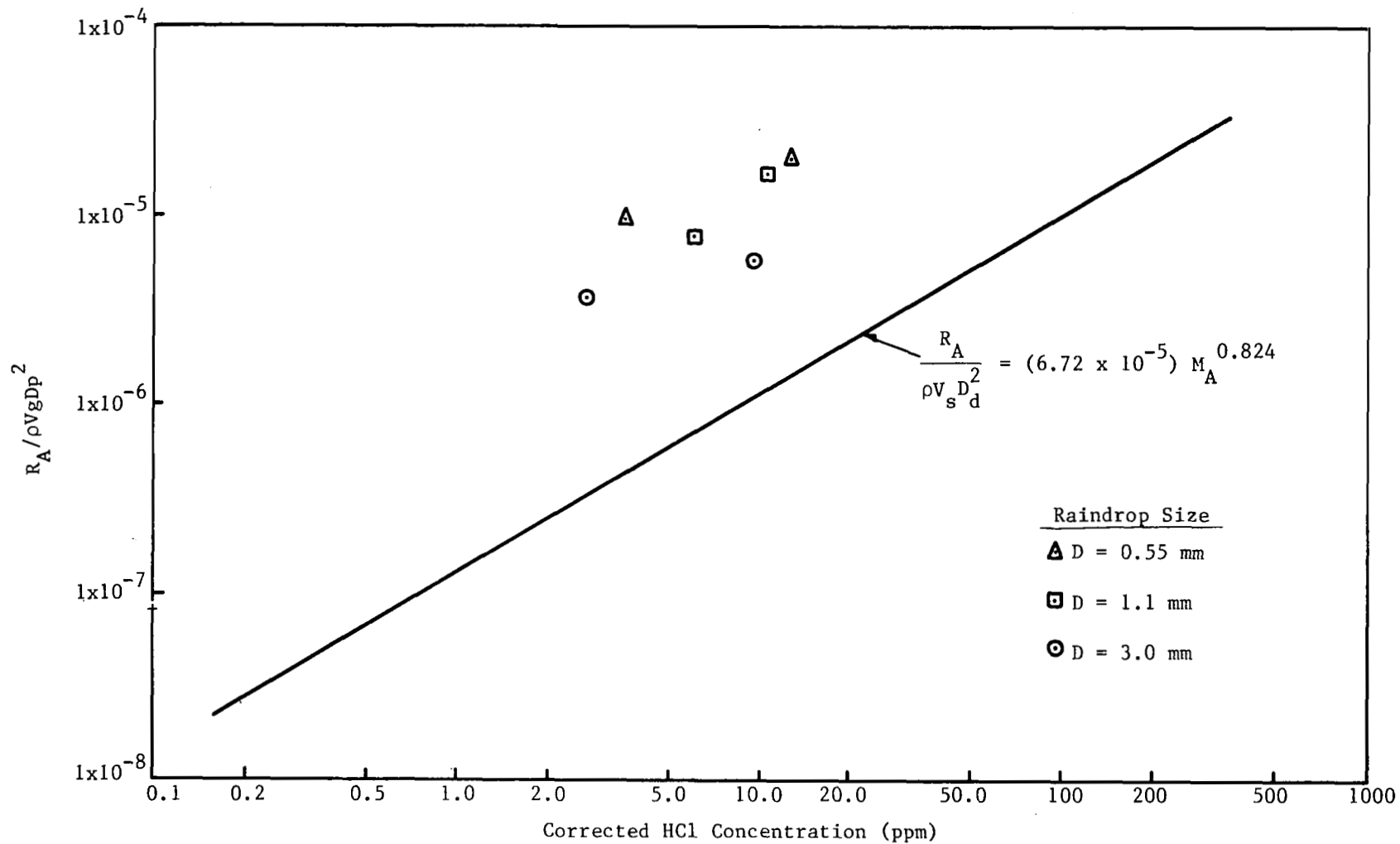


Figure A-1
 PURE HCl SCAVENGING DATA FOR MULTIPLE RAINDROP SIZES

REFERENCES

1. Pellett, G.L. "Washout of HCl and Application to Solid Rocket Exhaust Clouds", paper presented at the Precipitation Scavenging Symposium, University of Illinois at Urbana, Illinois (October 14-18, 1974).
2. Knutson, E.O.; Fenton, D.L., "Atmospheric Scavenging of Hydrochloric Acid, "NASA CR-2598, George C. Marshall Space Flight Center, Alabama, IIT Research Inst., Chicago, Ill. (August 1975).
3. Dumbauld, R.K.; Bjorkland, J.R.; Bowers J.F.; "NASA/MSFC Multilayer Diffusion Models and Computer Program for Operational Prediction of Toxic Fuel Hazards", H.E. Cramer Co., Report No. TR-73-301-02 to the George C. Marshall Flight Center, (March 1973).
4. Ranade, M.B., "Sampling Interface for Quantitative Transport of Aerosols", Final Report, IITRI, EPA Contract No. 68-02-0579, Chem. and Physics Lab., EPA, Research Triangle Park, N.C.
5. Strand, Leon, Private Communication, Jet Propulsion Laboratory, Pasadena, California, June 9, 1977.
6. Lord Rayleigh, *Philosoph. Mag.*, 36 (1878).
7. Strom, L., *Rev. Sci. Instruments*, 35: 778 (1969).
8. Berglund, R.N.; Liu, B.Y.H., *Environmental Sci. Technol.*, 7: 747 (1973).
9. Schneider, J.M.; Hendricks, C.D., *Rev. Sci. Instruments*, 35: 1349 (1964)
10. Wedding, J.B.; Stukel, J.J., "Operational Limits of Vibrating Orifice Aerosol Generator", *Environmental Sci. Technol.*, 8 (5): 456 (1974).
11. Gunn, R.; Kinzer, G.C., "The Theoretical Velocity of Fall for Water Droplets in Stagnant Air", *J. Meteor.*, 6: 243-248 (1949).
12. Knutson, E.O.; Fenton, D.L., "Atmospheric Scavenging of Hydrochloric Acid", NASA CR-2598, George C. Marshall Space Flight Center, Alabama, IIT Research Inst., Chicago, Ill. (August 1975).
13. Dawbarn, R., Private Communication, ARO Inc., Arnold Air Force Station, Tenn., May 18, 1976.
14. Sherwood, T.K., Pigford, R.L., and Wike, C.R., Mass Transfer, McGraw-Hill, USA, pp. 81-83 (1975).
15. Fuchs, N.A., The Mechanics of Aerosols, Pergamon Press, Oxford pp. 184, 204-206 (1964)

REFERENCE (cont.)

16. Gillespie, G.R.; Johnstone, H.F., "Particle Size Distribution in Some Hygroscopic Aerosols", Chem. Engr. Prog., pp. 74F-80F, Feb. 1955.
17. Fenton, D.L.; Ranade M.B., "Aerosol Formation Threshold for the HCl-Water Vapor System", Environmental Sci. and Technol., 10 (12): 1160-1162 (Nov. 1976).
18. Schem, C., Private Communication, Naval Air Propulsion Test Center, Trenton, New Jersey (October 19, 1976).
19. Marshall, J.S.; Palmer, W.M., "The Distribution of Raindrops with Size", J. Meteor., 5: 165-166 (1948).
20. Dingle, A.N.; Hardy, K.R., "The Description of Rain by Means of Sequential Raindrop Size Distribution", Quart. J. Roy. Meteor. Soc., 88: 301-304 (1962).
21. Buchanan, P., M.D., presentation at "Environmental Effects Workshop", Atmospheric Diffusion/Environmental Effects Technical Task Team, ES43, NASA/Marshall Space Flight Center, Alabama (September 8, 1974).
22. Heck, W., private communication, North Carolina State University (September 8, 1976).
23. Lerman, S.; Taylor, O.C.; Darley, E.F., "Phytotoxicity of Hydrogen Chloride Gas with a short-term exposure", Atmospheric Environ., 10: 873-878 (1976).

1. REPORT NO. NASA CR-2997	2. GOVERNMENT ACCESSION NO.	3. RECIPIENT'S CATALOG NO.	
4. TITLE AND SUBTITLE Atmospheric Scavenging of Solid Rocket Exhaust Effluents		5. REPORT DATE April 1978	6. PERFORMING ORGANIZATION CODE
		8. PERFORMING ORGANIZATION REPORT #	
7. AUTHOR(S) Donald L. Fenton and Robert Y. Purcell		10. WORK UNIT NO. M-251	11. CONTRACT OR GRANT NO. NAS8-31947
9. PERFORMING ORGANIZATION NAME AND ADDRESS IIT Research Institute 10 West 35th Street Chicago, Illinois 60616		13. TYPE OF REPORT & PERIOD COVERED Contractor	
		14. SPONSORING AGENCY CODE	
12. SPONSORING AGENCY NAME AND ADDRESS National Aeronautics and Space Administration Washington, D. C. 20546		15. SUPPLEMENTARY NOTES Prepared under the technical monitorship of Dr. J. B. Stephens, Environmental Effects Task Team Leader, Atmospheric Sciences Division, Space Sciences Laboratory, NASA/MSFC	
16. ABSTRACT Solid propellant rocket exhaust was directly utilized to ascertain raindrop scavenging rates for hydrogen chloride. The airborne HCl concentration varied from 0.2 to 10.0 ppm, and the raindrop sizes tested included 0.55 mm, 1.1 mm, and 3.0 mm. Two chambers were used to conduct the experiments — a large, rigid-walled, spherical chamber stored the exhaust constituents, while the smaller chamber housing all the experiments was charged as required with rocket exhaust HCl. The washout coefficient for rocket exhaust HCl scavenging as determined empirically is $\Lambda = (5.12 \times 10^{-5}) M_A^{0.176} R^{0.773}$ where M_A is the mass concentration of HCl (g/m^3) and R is the rainfall intensity (mm/hr). The washout coefficient is noted to display a slight dependence on the HCl concentration. Surface uptake experiments demonstrated an HCl concentration dependence for distilled water. Sea water and brackish water HCl uptake was below the detection limit of the chlorine-ion analysis technique used. Plant-life HCl uptake experiments were limited to corn and soy beans. Plant age effectively correlated the HCl uptake data. Metallic corrosion was not significant for single 20-minute exposures to the exhaust HCl under varying relative humidity. Characterization of the aluminum oxide particles substantiated the similarity between the constituents of the small-scale rocket (227 g) and the full-size vehicles. Also a single aluminum oxide scavenging experiment, conducted with the 1.1 mm droplets, tentatively suggests that large numbers of submicron particles were collected.			
17. KEY WORDS Environmental Scavenging		18. DISTRIBUTION STATEMENT Category 45	
19. SECURITY CLASSIF. (of this report) Unclassified	20. SECURITY CLASSIF. (of this page) Unclassified	21. NO. OF PAGES 83	22. PRICE \$6.00

* For sale by the National Technical Information Service, Springfield, Virginia 22161